J Atmos Chem (2017) 74:423–450
DOI 10.1007/s10874-016-9350-8

Assessment of $PM_{2.5}$ chemical compositions in Delhi: primary vs secondary emissions and contribution to light extinction coefficient and visibility degradation

U.C. Dumka[1,2] · **S. Tiwari**[3] · **D.G. Kaskaoutis**[4] · **P.K. Hopke**[5] · **Jagvir Singh**[6] · **A.K. Srivastava**[3] · **D.S. Bisht**[3] · **S.D. Attri**[7] · **S. Tyagi**[8] · **A. Misra**[8] · **G.S. Munawar Pasha**[9]

Received: 23 February 2016 / Accepted: 1 November 2016 /
Published online: 15 November 2016

Abstract Haze-fog conditions over northern India are associated with visibility degradation and severe attenuation of solar radiation by airborne particles with various chemical compositions. $PM_{2.5}$ samples have been collected in Delhi, India from December 2011 to November 2012 and analyzed for carbonaceous and inorganic species. PM_{10} measurements were made simultaneously such that $PM_{10-2.5}$ could be estimated by difference. This study analyzes the temporal variation of $PM_{2.5}$ and carbonaceous particles (CP), focusing on identification of the primary and secondary aerosol emissions, estimations of light extinction coefficient (b_{ext}) and

✉ U.C. Dumka
dumka@aries.res.in; ucdumka@gmail.com

[1] Aryabhatta Research Institute of Observational Sciences (ARIES), Nainital, Uttarakhand 263 001, India

[2] Shanghai Key Laboratory of Atmospheric Particle Pollution and Prevention, Department of Environmental Science and Engineering, Institute of Atmospheric Sciences, Fudan University, Shanghai 200 433, China

[3] Indian Institute of Tropical Meteorology, Branch, New Delhi 110 001, India

[4] Atmospheric Research Team, Institute for Environmental Research and Sustainable Development, National Observatory of Athens, -11810 Athens, GR, Greece

[5] Clarkson University, Box 5708, Potsdam, NY 13699-5708, USA

[6] Earth System Science Organization, Ministry of Earth Sciences, Delhi 110 003, India

[7] India Meteorological Department, New Delhi 110 003, India

[8] School of Vocational Studies & Applied Sciences, Gautam Buddha University 201 303, India

[9] College Ghosia College of Engineering Ramanagara, Karnataka 562159, India

the contributions by the major $PM_{2.5}$ chemical components. The annual mean concentrations of $PM_{2.5}$, organic carbon (OC), elemental carbon (EC) and $PM_{10–2.5}$ were found to be 153.6 ± 59.8, 33.5 ± 15.9, 6.9 ± 3.9 and 91.1 ± 99.9 μg m^{-3}, respectively. Total CP, secondary organic aerosols and major anions (e.g., SO_4^{2-} and NO_3^-) maximize during the post-monsoon and winter due to fossil fuel combustion and biomass burning. $PM_{10–2.5}$ is more abundant during the pre-monsoon and post-monsoon. The OC/EC varies from 2.45 to 9.26 (mean of 5.18 ± 1.47), indicating the influence of multiple combustion sources. The b_{ext} exhibits highest values (910 ± 280 and 1221 ± 371 Mm^{-1}) in post-monsoon and winter and lowest in monsoon (363 ± 110 and 457 ± 133 Mm^{-1}) as estimated via the original and revised IMPROVE algorithms, respectively. Organic matter (OM =1.6 × OC) accounts for ~39 % and ~48 % of the b_{ext}, followed by $(NH_4)_2SO_4$ (~21 % and ~24 %) and EC (~13 % and ~10 %), according to the original and revised algorithms, respectively. The b_{ext} estimates via the two IMPROVE versions are highly correlated (R^2 = 0.95, root mean square error = 38 % and mean bias error = 28 %) and are strongly related to visibility impairment (r = −0.72), mostly associated with anthropogenic rather than natural PM contributions. Therefore, reduction of CP and precursor gas emissions represents an urgent opportunity for air quality improvement across Delhi.

Keywords $PM_{2.5}$ · Carbonaceous aerosols · Primary/secondary emissions · Light extinction coefficient · Improve · Visibility · Delhi

1 Introduction

Particulate matter ($PM_{2.5}$, PM_{10}, $PM_{10–2.5}$) and gaseous air pollutants in urban environments play a vital role in air quality, visibility degradation, light extinction processes, etc. (Foyo-Moreno et al. 2014; Pateraki et al. 2014; Valenzuela et al. 2015; Khalil and Shaffie 2016). Especially over densely populated areas in the South and East Asia, visibility has significantly declined due to a dramatic increase in atmospheric particulate pollution (Wang and Shi 2010; Tiwari et al. 2014; Wang et al. 2015). Atmospheric light extinction is defined as the fractional loss of intensity in a solar light beam per unit distance due to extinction (scattering and absorption) by aerosol particles and gasses (Pitchford et al. 2007). The extinction aerosol coefficient (b_{ext}) is highly related to particle size and chemical composition (Badarinath et al. 2008; Huang et al. 2014) and can be measured by in-situ (e.g. Nephelometer, Aethalometer) and remote sensing (e.g. LIDAR) techniques or estimated based on aerosol mass and extinction efficiencies of various chemical constituents by assuming them as externally mixed particles (Cao et al. 2012; Wang et al. 2012; Zhang et al. 2013a; Tao et al. 2014; Shen et al. 2014).

Carbonaceous particles (CP) constitute a large fraction of the atmospheric aerosol with serious concerns about climate change, air pollution, visibility impairment and human health (e.g., Singh et al. 2014; Reddington et al. 2015). CP are composed of organic carbon (OC) and elemental carbon (EC), also known as equivalent black carbon (eBC). EC is a primary pollutant emitted from incomplete combustions of carbon-contained materials (Viana et al. 2007; Paraskevopoulou et al. 2014). It constitutes an important driver for global warming due to its strong absorbing efficiency (Novakov et al. 2005; Bond et al. 2013). In contrast, OC can be either released directly into the atmosphere (primary OC: POC) or produced from gas-to-particle reactions (secondary OC: SOC) (Bougiatioti et al. 2013). It is mostly scattering in

nature with an important role in the formation of urban haze (Gautam et al. 2007). However, it can contain significant amounts of light absorbing species termed Brown Carbon (Andreae and Gelencsér 2006). OC represents a mixture of many organic compounds (including polycyclic aromatic hydrocarbons, PAHs), some of which are mutagenic and/or carcinogenic (Smith et al. 2007; Li et al. 2008). A significant fraction of OC is water soluble (known as WSOC), with potential influence on chemical reactions and aerosol-cloud interactions (Decesari et al. 2000; Ram and Sarin 2011).

Due to their serious impact on atmospheric chemistry, monsoon circulation and climate, CP and ionic species have been of particular interest over the Indo-Gangetic Plains (IGP) during the last decade (Rengarajan et al. 2007; Behera and Sharma 2010a, 2010b; Ram et al. 2010a, b, Ram et al. 2012; Ram and Sarin 2011; Tiwari et al. 2013a, 2013b; Rastogi et al. 2014; Sharma et al. 2014; Srinivas and Sarin 2014; Bisht et al. 2015; Panda et al. 2016). These studies measured the chemical characterization of the $PM_{2.5}$, diagnostic ratios for identification of the aerosol source apportionment, and primary and secondary aerosol formation mechanisms. Other works have dealt with aerosol emission inventories (Streets et al. 2004; Lu et al. 2011) from different sources helping to understand the role of biomass burning. Venkataraman et al. (2005) examined the relative contributions of fossil-fuel combustion, biomass and biofuel burning to BC mass, which were estimated to ~25 %, 33 % and 42 %, respectively, whereas their contributions to OC were found to be ~13 %, 43 %, and 44 %, respectively. As a consequence, different kinds of burning, along with atmospheric mixing and long-range transport, are responsible for changing atmospheric composition over India, affecting aerosol-cloud interactions, monsoon circulation, and climate (Ganguly et al. 2012; Nair et al. 2012).

Many studies summarized by Bisht et al. (2015), analyzed the CP, $PM_{2.5,}$ and PM_{10} concentrations and examined their influence on air quality over Delhi. Bisht et al. (2015) using $PM_{2.5}$ chemical analyses for CP, SO_4^{2-} and NO_3^- examined the seasonal evolution of their daytime and night-time concentrations, the contributions to $PM_{2.5}$ mass and their association with the meteorological conditions and long-range transport over Delhi during January to December 2012. The current work aims to further contribute to the findings by Bisht et al. (2015) by estimating the b_{ext} for Delhi based on chemical analysis of $PM_{2.5}$ samples by means of the original and revised IMPROVE algorithms (Pitchford et al. 2007; IMPROVE 2011). $PM_{2.5}$ samples were collected from December 2011 to November 2012 covering periods with different atmospheric circulation patterns, emission rates, and aerosol characteristics. The main objectives of the study are: (i) to analyse the temporal variability of $PM_{2.5}$ and CP in comparison with Bisht et al. (2015), (ii), to assess the primary and secondary aerosol emissions, (iii) to investigate the temporal evolution of b_{ext} and the contributions of individual components of $PM_{2.5}$ on it, (iv) to examine the correspondence of b_{ext} to visibility degradation over Delhi and, (v) to compare the results obtained from the original and revised IMPROVE algorithms.

2 Experimental details and methodology

2.1 Site description

$PM_{2.5}$ samples were collected on the rooftop of a building (15 m above ground level) on the premises of the Indian Institute of Tropical Meteorology (IITM), New Delhi during December 2011 to November 2012. The sampling site is surrounded by heavy roadside traffic, small, medium and large-scale industries and agricultural fields towards the south, which along with

long-range transported and road re-suspended dust are the major sources of aerosols and pollutants over Delhi (Srivastava et al. 2012; Tiwari et al. 2013a, 2013b). Air masses from northwest directions dominate during post-monsoon (October – November) and winter (December–February) shifting to the west during pre-monsoon (March–June) and then to southeast during the rainy summer monsoon (July–September), thus controlling the PM concentrations and characteristics across Delhi (Lodhi et al. 2013; Bisht et al. 2015).

2.2 Instrumentation and chemical analysis of $PM_{2.5}$

For the current study, 75 $PM_{2.5}$ samples (~5–7 samples per month with duration of 10–12 h per day during the daytime) were collected from December 2011 to November 2012. Although the study period is similar to that (January – December 2012) used in Bisht et al. (2015), the sampling days and duration are different allowing us for a direct comparison of the $PM_{2.5}$ and CP concentrations between the two studies. $PM_{2.5}$ sampling was conducted over 10–12 h per day and only during the daytime. Thus, there can be concerns about their representativeness and this approach could also mean that some aerosol/pollution events may not have been caught in the presented time series. The $PM_{2.5}$ samples were collected on quartz fiber filters using APM 550 samplers (Envirotech Pvt. Ltd., India; http://www.envirotechindia.com/). The filters were subjected to 24-h desiccation before and after the sampling for the removal of moisture. Then, they were weighted using an electronic microbalance (Model GR202, A&D Company Ltd. Japan) with high resolution (0.001 mg) and accuracy. The particle concentrations were determined gravimetrically by the difference in their weights before and after the sampling.

The exposed filters were analyzed for CP (OC and EC) mass concentrations by a thermal/optical OC/EC analyzer (Sunset Laboratory Inc. Model 4 L; http://www.sunlab.com) using the NIOSH 5040 (National Institute for Occupational Safety and Health) thermo-optical transmittance protocol (Birch and Cary 1986). A punch from the filter (2.1 cm^2) is stepwise heated in an inert (100 % He) atmosphere, followed by heating in an oxidizing medium (~10 % O_2 and 90 % He). The carbon evolved during the processes is oxidized to CO_2 and converted to methane (CH_4) that is measured via a suitable detector. The detector transmits a 678 nm laser beam through the sampled filter. The return of the transmitted signal to its initial value on the thermograph is taken as a split line between OC and EC. The amount of carbon fraction evolved before the split line is defined as OC and after the split line as EC. A similar process has been followed using a blank filter to determine the detection limit of OC and EC in order to correct for the contribution of OC from the quartz filters. More details about the analysis of OC and EC mass concentrations are presented in previous papers (Tiwari et al. 2012, 2014; Bisht et al. 2015).

The concentrations of several ionic species (SO_4^{2-}, NO_3^-, F^- and NH_4^+) are necessary for the estimations of b_{ext} via the IMPROVE algorithm. They were analyzed using an Ion Chromatograph (DIONEX-2000, RFIC, USA). The anions (SO_4^{2-}, NO_3^- and F^-) were analyzed by the Ion Chromatograph (model IC-2000) using an IonPac-AS15 analytical column with an ASRS ultra II 2 mm micro-membrane suppressor. The eluent was 38 mM potassium hydroxide/1.7 mM sodium bicarbonate. Triple deionized water was used as the regenerator. The system has a detection limit of ~0.02 ppm. Field blanks were also analyzed using similar procedures as filter samples and found to be below the detection limits. The glassware used in the extraction and analysis were soaked in diluted nitric acid overnight and washed thoroughly with tripled distilled and deionized water to remove any adhered impurities. Due to technical problems with the instrument, cations were not analyzed in the present study. The NH_4^+ concentration was measured by the indophenols-blue method using a

Spectronic-20D (Thermospectronic) spectrometer. Further details about the analysis of water-soluble inorganic ions are presented in previous papers (Ram et al. 2010a; Tiwari et al. 2009, 2012; Bisht et al. 2015).

A Chemiluminescence NO-NO_2-NO_x analyzer (Model 42i Thermo Electron Corporation, USA) was used for NO_X measurements. Continuous PM_{10} measurements were also made at IITM using a beta attenuation monitor (C_{14} BETA; Thermo Andersen, USA) (Tiwari et al. 2013a). The PM_{10} concentrations were averaged to the same time intervals as the integrated $PM_{2.5}$ samples so that the coarse particle mass ($PM_{10-2.5}$) could be calculated for later use in the b_{ext} estimations.

Meteorological parameters (e.g. temperature, relative humidity (RH), wind speed, and direction) and horizontal visibility records were obtained from the India Meteorological Department (IMD), New Delhi, located in close proximity (~500 m) to the sampling site. Additional information about the mixing height (MH) over Delhi was obtained from the HYSPLIT model (http://www.arl.noaa.gov/ready.html; Draxler and Rolph 2016). The $PM_{2.5}$ concentrations, CP, ionic species and b_{ext} are compared with visibility and MH, while the detailed investigation of the influence of the meteorological parameters, air masses and boundary-layer dynamics on the CP and ionic species concentrations was presented by Bisht et al. (2015).

2.3 Estimation of extinction coefficient

An initial estimation of b_{ext} was made using the original version of the Interagency Monitoring of Protected Visual Environment (IMPROVE) algorithm (Pitchford et al. 2007; IMPROVE 2011). The IMPROVE algorithm was initially adopted by the U.S. Environmental Protection Agency (EPA) for solar-light extinction estimations and to set a measure of the haze levels to provide a basis for their reduction (Pitchford et al. 2007). The algorithm has been widely used over the globe (Cao et al. 2012; Zhang et al. 2013a; Tao et al. 2014; Shen et al. 2014). In the present work, the original IMPROVE algorithm was initially used after some small modifications as:

$$b_{ext} = 3 \times f(RH) \times \{[AS] + [AN]\} + 4 \times [OM] + 10 \times [LAC] + 0.6 \times [CM] + 0.161 \times [\text{Nitrogen Dioxide}] + [\text{Fine Soil}] + 10 \quad (1)$$

where f(RH) is the hygroscopic growth term as a function of RH (Malm and Day 2001); daily-averaged RH values during the sampling periods were used to determine f(RH), which may underestimate the aerosol light scattering. The [AS], [AN], [OM], [LAC], [CM] and [Fine Soil] are the mass concentrations of ammonium sulfate (AS = (0.944) × [NH_4^+] + (1.02) × [SO_4^{2-}]), ammonium nitrate (AN = (1.29) × [NO_3^-]), organic matter, light absorbing carbon, coarse mass, and soil, respectively, while the value of 10 corresponds to the Rayleigh scattering, which is considered independent from the site elevation and meteorological conditions. Eq. (1) also assumes zero absorption from the atmospheric gasses (i.e. O_2, N_2) and particles such as sulfate, nitrate, and OM, while the light extinction contributed by any individual component can be estimated as separate term considering the particles as externally mixed (Pitchford et al. 2007). The unit of b_{ext} is in Mm^{-1} (= 10^{-6} m^{-1}), the mass concentrations of the chemical species are expressed in μg m^{-3}, while f(RH) is unitless. B_{ext} is estimated at 550 nm, which is traditionally used for visibility protection applications to characterize the light extinction (Pitchford et al. 2007). The measured SO_4^{2-} and NO_3^- ionic concentrations are associated with the ammonium salts as $(NH_4)_2SO_4$ and NH_4NO_3, respectively in Eq. (1).

The LAC corresponds to the measured EC concentration, while the CM to the coarse mode ($PM_{10-2.5}$) concentration as described in section 2.2. Based on the previous OM vs OC relationships over IGP (Ram and Sarin 2015 and references therein), the mass concentration of OM is estimated as OC × 1.6, correcting the OC mass for other elements (hydrogen, oxygen, nitrogen) associated with the OC molecules. Therefore, Eq. (1) uses the factor 1.6 instead of 1.4 in the original IMPROVE algorithm for the mean ratio of OM to measured OC. Furthermore, Eq. (1) involves the absorption by NO_2, which is neglected in the original IMPROVE algorithm. The soil fraction was estimated from the F^- mass assuming a global crustal abundance of 3.5 % (Taylor and McLennan 1985) using the equation:

$$[\text{Soil}] = \left(\frac{1}{0.035}\right) \times [F^-] \ = (28.57) \times [F^-] \tag{2}$$

(2)

The F^- concentration for soil mass estimations was used because of unavailability of Al^{3+}, Ca^{2+}, Mg^{+2} or Fe^{2+}, which are much more abundant than F^- in the soil samples (Guinot et al. 2007), this assumption introduces some additional uncertainty into the calculation of the reconstructed fine mass (RCFM) and in the estimations of b_{ext}, taking also into account that F^- can have anthropogenic sources as well (Kumar et al. 2010; Saxena et al. 2014).

In addition, b_{ext} estimations across Delhi were also performed via the revised IMPROVE algorithm, which is well documented in Pitchford et al. (2007), as:

$$\begin{aligned} b_{ext} = {} & 2.2 \times f_s(RH) \times [\text{Small Sulfate}] + 4.8 \times f_L(RH) \times [\text{Large Sulfate}] + 2.4 \\ & \times f_s(RH) \times [\text{Small Nitrate}] + 5.1 \times f_L(RH) \times [\text{Large Nitrate}] + 2.8 \\ & \times [\text{Small Organic Mass}] + 6.1 \times [\text{Large Organice Mass}] + 10 \\ & \times [\text{Elemental Carbon}] + 1 \times [\text{Fine Soil}] + 1.7 \times f_{ss}(RH) \times [Sea\ Salt = 1.8 * Cl^-] \\ & + 0.6 \times [\text{Coarse Mass}] + \text{Rayleigh Scattering (Site Specific)} + 0.33 \\ & \times [NO_2(ppb)] \end{aligned} \tag{3}$$

Compared to Eq. (1), the revised IMPROVE algorithm takes into consideration three components (i.e. sulfate, nitrate and organic mass) that are split into small and large particle-size modes, while for sulfate and nitrate the algorithm includes different growth factor terms for the large and small modes for less biased b_{ext} estimations as:

$$[\text{Large } Sulfate] = \frac{[\text{Total Sulfate}]^2}{20}, for\ [\text{Total Sulfate}] < 20\ \mu g\ m^{-3} \tag{4}$$

$$[\text{Large Sulfate}] = [\text{Total Sulfate}], for\ [\text{Total Sulfate}] \geq 20\ \mu g\ m^{-3} \tag{5}$$

$$[\text{Small Sulfate}] = [\text{Total Sulfate}] - [\text{Large Sulf}ate] \tag{6}$$

Similar differentiation and a threshold of 20 μg m^{-3} exists for the nitrate and OM. The revised algorithm considers variable dry-mass extinction efficiencies that are smaller (larger) than the original values for the small (large) particle size modes. This change was made to account for the growth of dry particles results in size ranges with higher scattering efficiencies under more turbid conditions (Pitchford et al. 2007). Furthermore, the Rayleigh scattering

component was calculated for each daily sample taking into consideration the elevation of the site and the annual average temperature. The sea-salt component was neglected in the present study due to unavailability of Cl^- measurements for its consideration. However, this deletion is expected to produce little bias since sea salt is mostly important in coastal environments. Behera and Sharma (2010b) found negligible sea-salt amount over Kanpur in the central IGP. The ratio between the OM and measured OC was fixed at 1.6 in the initial calculation. It has been modified to 1.8 in the revised IMPROVE algorithm. The $f_S(RH)$ and $f_L(RH)$ were taken from Pitchford et al. (2007), for the averaged RH values during the sampling periods, while the remaining components, i.e., EC, fine soil and coarse mass were calculated identically in the revised algorithm compared to the original calculations.

3 Results and discussion

3.1 $PM_{2.5}$ and carbonaceous aerosol concentrations

Before examining the primary and secondary aerosol emissions and the estimations of the b_{ext} via chemical analysis of $PM_{2.5}$, the temporal variability of $PM_{2.5}$ and CP concentrations is analyzed in this section. The mean (December 2011 to November 2012) $PM_{2.5}$ mass concentration at the measuring site was 153.6 ± 59.8 μg m^{-3} varying from ~65.0 to 289.7 μg m^{-3} compared to 171.6 ± 51.6 μg m^{-3} obtained from 90 $PM_{2.5}$ samples during January – December 2012 (Bisht et al. 2015). This difference is attributed to the fact that the current work uses only daytime $PM_{2.5}$ samples, which are generally lower than the nighttime ones, especially during post-monsoon and winter (Bisht et al. 2015). Table 1 summarizes the seasonal-mean mass concentrations of $PM_{2.5}$ and CP, while the daily concentrations are presented in Fig. 1.

The $PM_{2.5}$ annual and seasonal means exceed the National Ambient Air Quality Standard (NAAQS; http://www.cpcb.nic.in/National-Ambient-Air-Quality-Standards.php) of 40 μg m^{-3} and are far beyond the annual average limits of 12 μg m^{-3} established by the United States Environmental Protection Agency (USEPA; http://www.epa.gov/air/criteria.html) and the 24-h limits (25 μg m^{-3} not to be exceeded for more than 35 days in a year) of the European Union legislation (Directive 2008/50/EC 20). On a monthly mean basis, 241.9 ± 41.6 μg m^{-3} was observed in November 2012 due to substantial agricultural crop residue burning in northwest India (Kaskaoutis et al. 2014). Minimum $PM_{2.5}$ (84.6 ± 13.6 μg m^{-3}) was observed in August 2012 because of washout similar to Bisht et al. (2015). The highest $PM_{2.5}$ concentrations during post-monsoon and winter (Table 1) are attributed to increased agricultural burning, biofuel and solid waste burning for heating purposes as well as the lower mixing layer height trapping the pollutants near the ground (Hÿvarinen et al. 2011; Rastogi et al. 2014; Bisht et al. 2015).

Prominent peaks in $PM_{2.5}$ were mostly observed during the pre-monsoon (Fig. 1), associated with transported dust plumes from the Thar Desert, Arabian Peninsula, and other areas in western Asia that affect ground-level $PM_{2.5}$ concentrations (Tiwari et al. 2013b). High $PM_{2.5}$ concentrations have been reported over the whole IGP [e.g. Agra: 90.2 ± 7.2 μg m^{-3} (Pipal et al. 2011); Delhi: 148.4 ± 67.0 μg m^{-3} (Dey et al. 2012), 97 ± 56 μg m^{-3} (Tiwari et al. 2009), 122.3 ± 90.7 μg m^{-3}, (Tiwari et al. 2013a), 123 ± 87 μg m^{-3}, (Guttikunda and Calori 2013); Lucknow: 101.1 ± 22.5 μg m^{-3}, (Pandey et al. 2012); Kanpur: 95 μg m^{-3} (Sharma and Maloo 2005); Kharagpur: 89.7 ± 33.7 μg m^{-3}, (Srinivas and Sarin 2014), among many others], which are comparable in magnitude with the current concentrations.

Table 1 Seasonal-mean concentrations of $PM_{2.5,}$ carbonaceous aerosols (OC, OM, and EC) and coarse particles ($PM_{10–2.5}$) over Delhi during December 2011 – November 2012. [Organic Matter: OC*1.6; total carbonaceous particles: TCP = OM + EC]

Seasons	$PM_{2.5}$ (μg m^{-3})	OC (μg m^{-3})	OM[a] (μg m^{-3})	EC (μg m^{-3})	OC/EC	TCP (μg m^{-3})	TCP/$PM_{2.5}$ (%)	$PM_{10–2.5}$ (μg m^{-3})
Winter	229.24 ± 18.11	55.53 ± 7.12	88.84 ± 11.39	10.41 ± 1.97	5.44 ± 0.71	99.25 ± 13.04	43.38 ± 4.99	74.99 ± 43.23
Pre-mon	143.46 ± 36.66	27.13 ± 9.19	43.41 ± 14.70	5.99 ± 3.13	4.95 ± 1.53	49.40 ± 17.07	35.46 ± 11.33	113.42 ± 117.14
Monsoon	95.96 ± 23.13	22.78 ± 8.03	36.45 ± 12.85	4.19 ± 1.56	5.66 ± 1.68	40.64 ± 13.94	42.16 ± 9.51	40.55 ± 28.62
Post-mon	222.81 ± 54.56	51.71 ± 13.25	82.74 ± 21.21	12.90 ± 4.54	4.24 ± 0.83	95.65 ± 24.74	43.51 ± 7.52	169.25 ± 139.57
Average	153.57 ± 59.75	33.51 ± 15.89	53.61 ± 25.43	6.96 ± 3.97	5.18 ± 1.47	60.57 ± 28.84	39.57 ± 10.26	91.05 ± 99.94

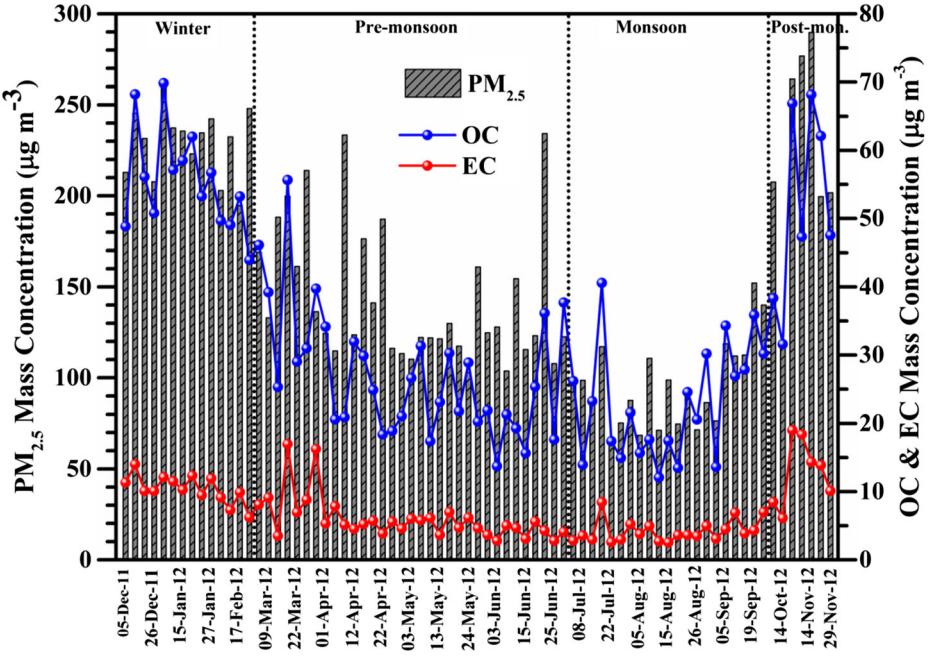

Fig. 1 Daily variability of $PM_{2.5}$, OC and EC mass concentrations on the 75 days with $PM_{2.5}$ samples in Delhi during December 2011 – November 2012

A mean OC concentration of 33.5 ± 15.9 μg m^{-3} was found on an annual basis, varying from ~12.1 to 69.8 μg m^{-3} (Fig. 1). OC is the major contributor (~22 %) to $PM_{2.5}$ mass, comparable to results at urban European sites (Putaud et al. 2010). The EC concentration ranges between 2.5 and 19.0 μg m^{-3} (mean of 6.9 ± 3.9 μg m^{-3}) corresponding to ~5 % of the $PM_{2.5}$ mass. Bisht et al. (2015) reported very similar values for OC (37.7 ± 14.3 μg m^{-3}) and EC (7.8 ± 3.7 μg m^{-3}), with larger concentrations during night-time in all seasons. OC exhibits its highest concentration (59.6 ± 5.3 μg m^{-3}) in January and lowest (19.3 ± 5.4 μg m^{-3}) in August, whereas EC presents a November high (14.2 ± 2.9 μg m^{-3}) and an August low (3.9 ± 0.9 μg m^{-3}). Prior work in Delhi has found average OC in PM_{10} of 25.6 ± 12.5 μg m^{-3} and EC of 12.1 ± 6.8 μg m^{-3} in 86 samples collected between January 2013 and June 2014 with similar seasonal patterns to those observed in this study (Sharma et al. 2016). In a previous study in 2010, Sharma et al. (2014) reported average OC of 26.7 ± 9.2 μg m^{-3}, and EC of 6.1 ± 3.9 μg m^{-3}.

A near-zero intercept in the regression of EC against OC [EC = (0.21 ± 0.02)*OC – (0.06 ± 0.59), R^2 = 0.70] suggests negligible OC emissions from primary non-combustion sources, such as road re-suspended soil carbonates (Kamani et al. 2015), biogenic emissions, evaporation of fuel and solvents. This result differs from Kanpur, where an intercept of 5.76 was found (Behera and Sharma 2010b). The high concentrations of CP during late post-monsoon and winter (Table 1) are attributed to calm, stable atmospheric conditions and lower MH (Bisht et al. 2015), along more extensive fossil fuel and biofuel combustion for heating purposes, influence of transported smoke from agricultural burning, and fireworks during Diwali festival (Tiwari et al. 2012).

The OC/EC ratio is commonly used as an identification factor for the relative dominance between biomass/biofuel burning and fossil-fuel combustion (Turpin and Huntzicker 1995; Ram et al. 2010a; b; Pio et al. 2011; Panda et al. 2016). In the present study, the OC/EC varies from 2.45 to 9.26 (average: 5.18 ± 1.47) compared to 5.86 ± 0.99 in Bisht et al. (2015). It exhibited only a small seasonal variability from 4.24 ± 0.83 in the post-monsoon to 5.66 ± 1.68 in the monsoon (Table 1). These values are indicative of mixing of various carbonaceous sources, such as coal combustion, motor vehicle exhausts, agricultural burning, solid waste burning, industrial and thermal power plants emissions. More comparisons between OC, EC concentrations as well as OC/EC over Delhi and other cities in Asia can be seen in Bisht et al. (2015). Panda et al. (2016) report a winter only OC/EC ratio of 1.37 ± 0.16. However, their OC/EC analysis was performed with the IMPROVE protocol so that their EC values are likely to be a factor of 2 higher than with the NIOSH protocol (Chow et al. 2004). Thus, their OC/EC ratio is similar to the minimum value observed in this study. Sharma et al. (2014) found that OC/EC ratios varied from 3.8 to 5.8 in Delhi during 2010. Both of these studies examined PM_{10} using the IMPROVE protocol that typically measures more EC than the NIOSH protocol used in the present study.

During the study period, the total CP (TCP = 1.6 x OC + EC) varied from 22.0 to 126.1 μg m^{-3} (60.6 ± 28.8 μg m^{-3}) contributing ~39.6 % to the $PM_{2.5}$ mass, almost similar to that found in Athens (Mantas et al. 2014). Despite the large seasonality in the TCP concentrations (Table 1), the contributions to the $PM_{2.5}$ mass are similar (42–43.5 %) in all seasons, except in pre-monsoon when it is lower (35.5 %) due to enhanced contribution of dust (Lodhi et al. 2013), highlighting the serious role of CP in emission rates and atmospheric chemistry over Delhi.

3.2 Estimation of primary and secondary emissions

Secondary organic aerosol (SOA) is an important component of haze formation, visibility degradation, climate and health-related issues (Hoyle et al. 2011; Ram and Sarin 2011). However, the estimation of SOA is complicated because it is difficult to distinguish between SOA and oxidized POC (Robinson et al. 2007; Jimenez et al. 2009). An approach to estimating SOA is through the estimation of secondary organic carbon (SOC) using the EC tracer method (Turpin and Huntzicker 1995; Castro et al. 1999; Ram et al. 2008, Ram et al. 2010a, b; Behera and Sharma 2010b; Panda et al. 2016). The EC tracer method for POC, SOC, POA, and SOA estimates are as follows (Feng et al. 2009; Ram and Sarin 2011):

$$POC = (EC)_{\text{total}} \times \left(\frac{OC}{EC}\right)_{\text{primary}} \tag{7}$$

$$SOC = (OC)_{\text{total}} - POC \tag{8}$$

$$POA = 1.6 \times POC \tag{9}$$

$$SOA = 1.6 \times SOC \tag{10}$$

One of the major uncertainties in the estimations of POC and SOC is the estimation of $(OC/EC)_{primary}$ (Behera and Sharma 2010b). In order to determine the $(OC/EC)_{primary}$, we assume that the minimum OC/EC (2.45) represents the aerosol having negligible SOC (Castro

et al. 1999; Panda et al. 2016). This value is reasonable based on the limited other results available for Delhi (Sharma et al. 2014; Panda et al. 2016). Using this approach, the annual average concentrations of POC and SOC were estimated to be 17.0 ± 9.7 μg m^{-3} and 16.7 ± 9.2 μg m^{-3} (~50.6 % and 49.4 % of OC mass), respectively, indicating equal contributions from POC and SOC to the total OC mass over Delhi (Table 2).

The cumulative contributions of POC and SOC to the daily $PM_{2.5}$ samples along with the SOC/OC (%) ratios are shown in Fig. 2a, while Fig. 2b shows the daily variation of NO_2 and SOA concentration and its contribution to $PM_{2.5}$ from December 2011 to November 2012. The POC emissions dominate during post-monsoon due to frequent and extended agricultural burning in NW IGP, while SOC and SOA formations and % contributions to OC and $PM_{2.5}$ dominate during winter (Figs. 2a, b, Table 2). Feng et al. (2009) found SOC/OC of the order of 18–19 % for urban and 23–25 % for rural sites in China. These values are much lower than the SOC formation observed in Delhi. Similarly, high POA emissions during post-monsoon and winter are due to agricultural crop residue burning, domestic biofuel and waste burning for heating (Chen et al. 2006).

The relative (%) contributions of POC, SOC, and EC to the total carbon (TC = EC + OC) are illustrated in Fig. 3 on a seasonal basis, revealing a significant SOC contribution ranging from 31.1 % in post-monsoon to 46.4 % in monsoon. The POC accounts for 48.9 % of the TC during post-monsoon, also associated with the largest fraction (20 %) of EC due to large-scale agricultural burning in Punjab resulting in transported smoke plumes over Delhi during October to November 2012 (Kaskaoutis et al. 2014). Significant fractions of POC (43.8 %) and EC (17.9 %) are also found during pre-monsoon attributed to wheat crop residue burning in NW IGP and forest fires in Himalayan foothills (Kumar et al. 2011; Vadrevu et al. 2012) although with lower TC concentrations (Fig. 3). The decrease in combustion activities and open fires during monsoon, the dilution of carbonaceous aerosols due to the increasing MH (Bisht et al. 2015) and the precipitation washout lead to the lowest TC concentration (27.0 ± 9.1 μg m^{-3}), EC and POC % contributions (Fig. 3). On an annual average, POC, SOC, and EC account for 42 %, 41 %, and 17 %, respectively of the Delhi TC.

3.3 Inorganic species

The concentrations of the ionic species (SO_4^{2-}, NO_3^-, F^- and NH_4^+) are plotted in Fig. 4 (box and whisker charts) along with $PM_{2.5}$, CP, and NO_2 for a direct comparison between them. The average concentrations of SO_4^{2-}, NO_3^-, NH_4^+ and F^- are 19.1 ± 12.5, 8.9 ± 8.6, 5.8 ± 3.0 and 1.2 ± 1.1 μg m^{-3}, respectively indicating large contributions of sulphate and nitrate to PM in Delhi, although their concentrations are lower than those reported by Bisht et al. (2015). On a

Table 2 Seasonal-mean concentrations of estimated POC, SOC and SOA, along with fractions of SOC/OC and SOA/$PM_{2.5}$ over Delhi during December 2001–November 2012

Seasons	POC (μg m^{-3})	SOC (μg m^{-3})	SOC/OC (%)	SOA (μg m^{-3})	SOA/$PM_{2.5}$ (%)
Winter	25.51 ± 4.82	30.01 ± 4.21	54.24 ± 5.62	48.02 ± 6.73	20.94 ± 2.29
Pre-mon	14.68 ± 7.67	12.84 ± 6.27	47.23 ± 14.91	20.55 ± 10.03	14.77 ± 7.38
Monsoon	10.26 ± 3.82	12.52 ± 6.20	52.93 ± 13.15	20.03 ± 9.92	20.60 ± 8.18
Post-mon	31.62 ± 11.12	20.10 ± 9.08	39.31 ± 15.53	32.16 ± 14.53	15.44 ± 6.79
Average	17.04 ± 9.71	16.69 ± 9.22	49.42 ± 13.92	26.70 ± 14.76	17.66 ± 7.51

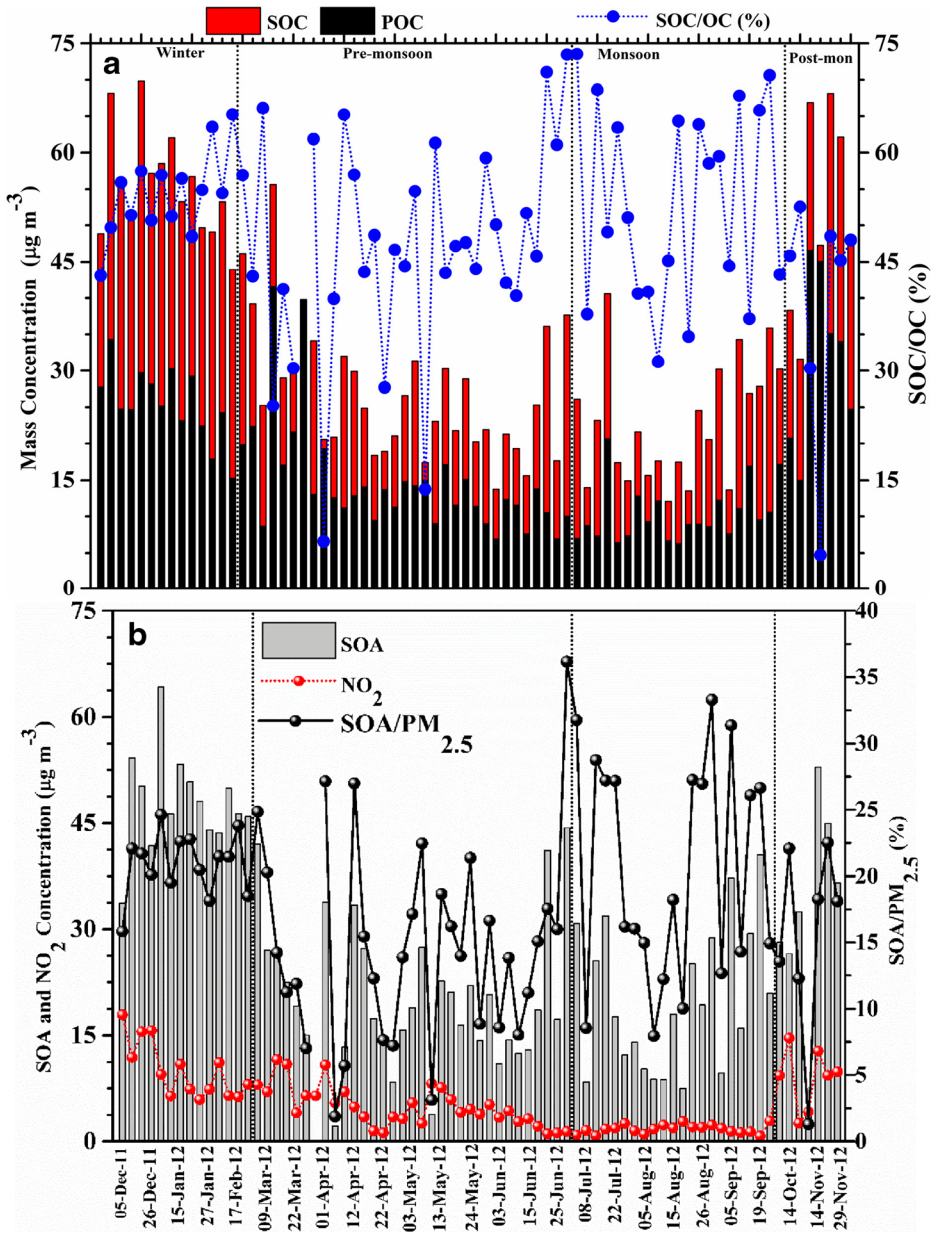

Fig. 2 Daily variability of (**a**) primary (POC), secondary (SOC) organic carbon emissions and SOC/OC and, (**b**) secondary organic aerosol (SOA), NO_2 concentrations and $SOA/PM_{2.5}$ for the 75 $PM_{2.5}$ samples in Delhi during December 2011–November 2012

monthly basis, the highest concentrations of SO_4^{2-} and NO_3^- were found to be 39.4 ± 13.8 μg m^{-3} and 29.6 ± 7.2 μg m^{-3}, respectively, in November, while the lowest values were in May (SO_4^{2-} = 9.7 ± 5.9 μg m^{-3}) and July (NO_3^- = 2.5 ± 1.4 μg m^{-3}). Ammonium and fluoride maximize in February (9.8 ± 2.8 μg m^{-3}, 2.6 ± 1.3 μg m^{-3}, respectively). The seasonality in SO_4^{2-} and NO_3^- for both daytime and nighttime concentrations is documented in Bisht et al. (2015).

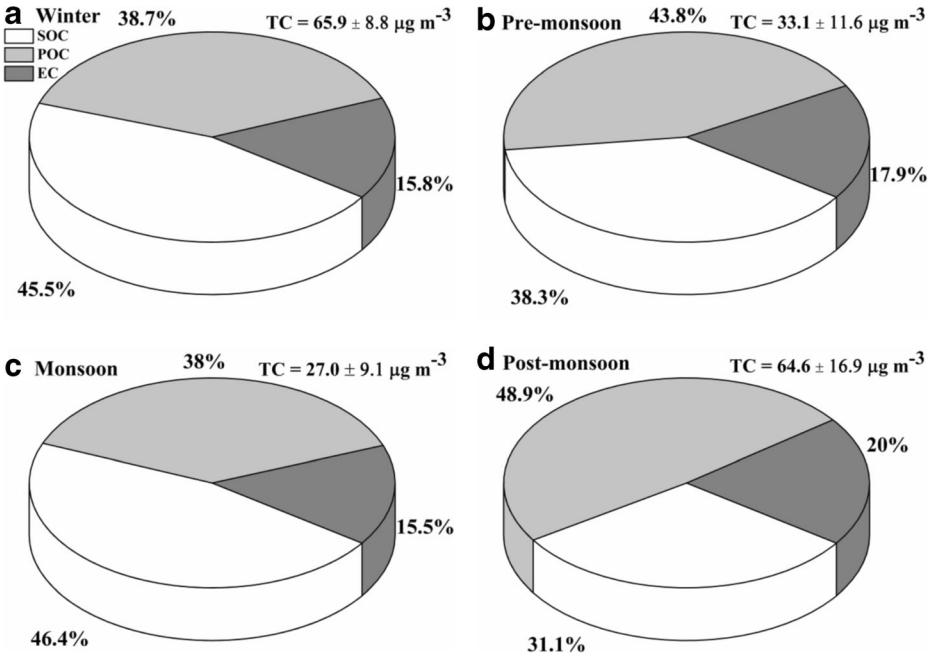

Fig. 3 Relative (%) contribution of POC, SOC and EC emissions to the total carbon (OC + EC) on seasonal basis. The seasonal-mean values of TC are also given

The ionic species and OC are light scattering-type aerosols, while EC is a strong absorber of solar light (Novakov et al. 2005; Bond et al. 2013). Beyond their climate-forcing response, the ratios between organic and inorganic species are commonly used for source identification and mixing processes in the atmosphere (Behera and Sharma 2010a; Srinivas and Sarin 2014). A linear regression analysis between $PM_{2.5}$, organic and inorganic components was performed and the Pearson correlation coefficients are summarized in Table 3. Statistically significant (95 % confidence level) positive correlations are found among the OC, EC, NO_3^- and SO_4^{2-} with $PM_{2.5}$, suggesting that all species and, more specifically OC and SO_4^{2-}, contribute significantly to $PM_{2.5}$. SO_4^{2-} is highly correlated (r = 0.79) with NO_3^- indicating similarity in the emission sources or reaction pathways, as also shown between OC and EC (r = 0.84) for vehicular and bio-fuel combustion processes. The NO_3^-/SO_4^{2-} ratio was calculated to be 0.46 varying between 0.25 (May) and 0.75 (November), similar to values seen by Sharma et al. (2016). Significant correlations were found between NO_3^- and OC (r = 0.66) and with EC (r = 0.64). EC is an indicator of vehicular emissions in urban environments as well as biomass burning while some of the nitrate and OC can be attributed to motor-vehicle emissions. SO_4^{2-} was correlated with OC (r = 0.67) and EC (r = 0.60) likely result from the condensation of OC on the sulfate particles (Tiwari et al., 2015). The sulfate-EC correlation is commonly observed in urban settings and likely to result from coagulation of EC emissions with the secondary sulfate particles. In contrast, NH_4^+ and F^- exhibit moderate-to-low correlations with the other components. Almost all of the chemical components exhibit significant negative correlations with the MH indicating that boundary-layer dynamics play an important role in air pollution levels in Delhi, as documented in Bisht et al. (2015). Therefore, the pollution levels maximize in the post-monsoon and

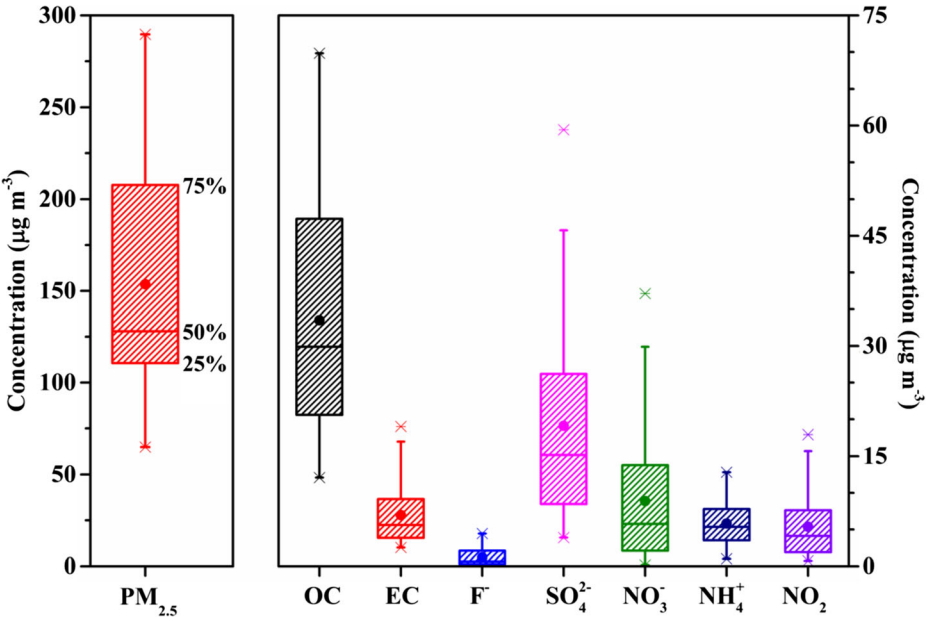

Fig. 4 Annual-mean concentrations (box and whisker plots) of $PM_{2.5}$, OC, EC, NO_2 and ionic species in Delhi during December 2011 – November 2012. The mean value stands for circle, the median with line (50 %), and vertical bars correspond to lower 5 % and upper 95 % of the values, while the asterisks represent the min and max values at each case

winter and during the early morning and late evening hours when the MH is low trapping the pollutants near the surface (Bisht et al. 2015).

3.4 Estimation of light extinction coefficient by measured chemical species

The light extinction coefficient (b_{ext}) was estimated across Delhi using the chemical composition data of the $PM_{2.5}$ samples using the original and revised IMPROVE algorithms (Pitchford et al. 2007). Before the b_{ext} estimations, $PM_{2.5}$ was reconstructed (simulated) based

Table 3 Correlation coefficient (r) between $PM_{2.5}$, carbonaceous aerosols and ionic species over Delhi from December 2011 to November 2012. [MH: Mixing height]. Values in bold (bold-asterisk) correspond to statistically significant correlations at 95 % (99 %) confidence level

	$PM_{2.5}$	OC	EC	F^-	NO_3^-	SO_4^{2-}	NH_4^+	MH
$PM_{2.5}$	1.00							
OC	0.82*	1.00						
EC	0.73*	0.84*	1.00					
F^-	0.34	0.31	0.19	1.00				
NO_3^-	0.75*	0.66	0.64	0.21	1.00			
SO_4^{2-}	0.85*	0.67	0.60	0.20	0.79	1.00		
NH_4^+	0.42	0.35	0.24	0.24	0.07	0.33	1.00	
MH	-0.48	-0.59	-0.51	-0.12	-0.50	-0.52	-0.09	1.00

on the measured chemical constituents. The RCFM (reconstructed fine mass) is computed as:

$$\mathrm{RCFM} = [AS] + [\mathrm{AN}] + [OM] + [LAC] + [\text{Fine Soil}] \quad (11)$$

where [AS] and [AN] are the concentrations of ammonium sulfate and ammonium nitrate, respectively, [OM] is the summary of primary and secondary organic matter, [LAC] is [EC], and fine soil is calculated by Eq. 2.

The measured and reconstructed $PM_{2.5}$ concentrations exhibit a satisfactory agreement (R^2 = 0.69) between the 75 samples (Fig. 5). In the most cases, RCFM underestimated the measured $PM_{2.5}$ with the largest underestimations reaching 60 %. In about 20 cases the measured and simulated $PM_{2.5}$ exhibit an excellent match with Root Mean Square Error (RMSE) <5 %, while the mean bias difference was found to be 23 %. The consideration of F^- as a representative of the soil component introduces large uncertainties in the calculation of RCFM and contributes to the underestimations shown in Fig. 5, since major soil components like Ca^{2+}, Mg^{2+}, Al^{+} as well as K^+, Na^+, Cl^- are not considered, whose summary was found to have an important fraction in the ionic composition over IGP (Ram et al. 2010a; Tiwari et al. 2016). Therefore, the large scatter of some data points and depart from the x = y line may be attributed to these issues.

The percentage (%) contribution of each component to the reconstructed $PM_{2.5}$ on a seasonal basis is shown in Fig. 6, revealing a clear dominance of OM (~40–44 %), followed by $(NH_4)_2SO_4$ (~18–21 %). The soil represents a significant fraction in winter, pre-monsoon and monsoon (~25–30 %), while its % contribution minimizes in post-monsoon (12 %) due to increasing in components associated with biomass burning. The large contribution of soil component during pre-monsoon and monsoon is attributed to enhanced dust activity and

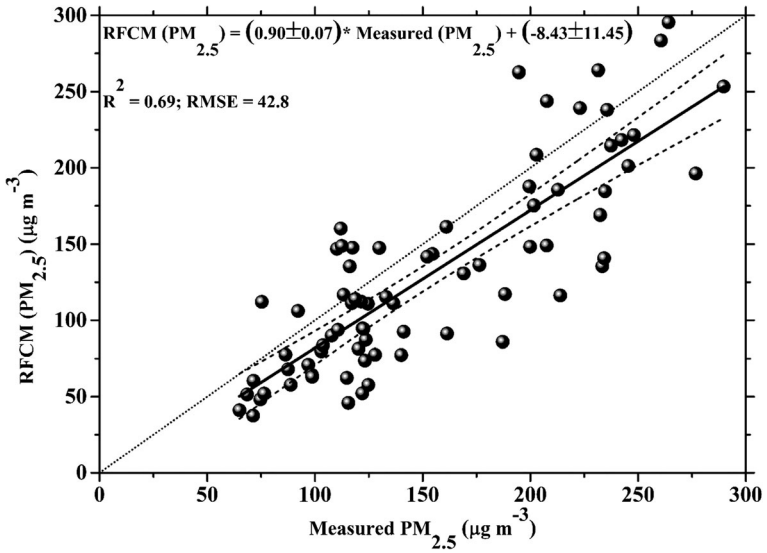

Fig. 5 Correlation between measured and reconstructed $PM_{2.5}$ concentrations in Delhi during December 2011 to November 2012. The dashed lines show the lower and upper 95 % confidence levels of the linear regression. The dotted line represents the 1–1

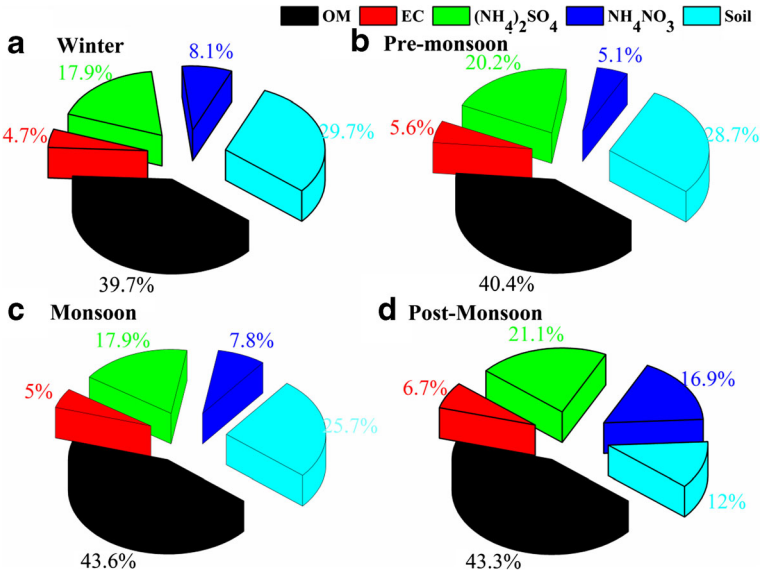

Fig. 6 Percentage (%) contribution of organic matter (OM), elemental carbon (EC), ammonium sulfate $(NH_4)_2SO_4$, ammonium nitrate NH_4NO_3 and soil in the $PM_{2.5}$ reconstructed mass on seasonal basis

transported dust plumes (Lodhi et al. 2013), while the large winter fraction may be mostly associated with road dust resuspension due to dry weather conditions (Behera and Sharma 2010b). F^- that was used for soil estimations (Eq. 2), may also have anthropogenic sources other than soil. The mean fractional contribution of EC remains nearly constant at 4.7 to 5.6 %, with the largest value (6.7 %) in the post-monsoon. During post-monsoon, NH_4NO_3 contributes ~17 % to the reconstructed $PM_{2.5}$ compared to 5–8 % in the other seasons (Fig. 6). Since Na^+ and Cl^- ions were not measured, the sea-salt mass contribution to $PM_{2.5}$ was neglected that can only contribute a small fraction of the underestimation of the RCFM (Fig. 5) since prior work found low concentrations of sea salt over central IGP (Behera and Sharma 2010b).

The daily variation of the estimated b_{ext} using the original and revised IMPROVE algorithms is plotted in Fig. 7a, b, respectively, as the cumulative absolute contributions of each chemical species. On a daily basis, b_{ext} varies from 196 to 1345 Mm^{-1} (mean of 545 ± 263 Mm^{-1}) for the original IMPROVE algorithm, and from 256 to 2189 Mm^{-1} (mean of 696 ± 380 Mm^{-1}) for the revised IMPROVE calculation. On a seasonal basis, b_{ext} is highest (910 ± 280 Mm^{-1}) in the post-monsoon, followed by winter (877 ± 180 Mm^{-1}), pre-monsoon (442 ± 109 Mm^{-1}) and monsoon (363 ± 110 Mm^{-1}) using the original IMPROVE, while the seasonality is slightly modified in the case of the revised IMPROVE with the highest b_{ext} occurring in winter (1222 ± 371 Mm^{-1}), followed by post-monsoon (1123 ± 308 Mm^{-1}), pre-monsoon (535 ± 145 Mm^{-1}) and monsoon (457 ± 133 Mm^{-1}). These b_{ext} values are significantly larger than those reported by Komppula et al. (2012) at Gual Pahari, about 20 km south of Delhi. However, Komppula et al. (2012) estimated the b_{ext} via LIDAR profiles as averaged values between 1 to 3 km from March 2008 to March 2009 and their results showed increasing b_{ext} within the first 1-km. Misra et al. (2012) reported b_{ext} values near the surface of 0.2–0.4 km^{-1} from May 2009 to September 2010 in Kanpur, which is much lower than the estimated b_{ext} over Delhi. However, the current estimates of b_{ext} are comparable to

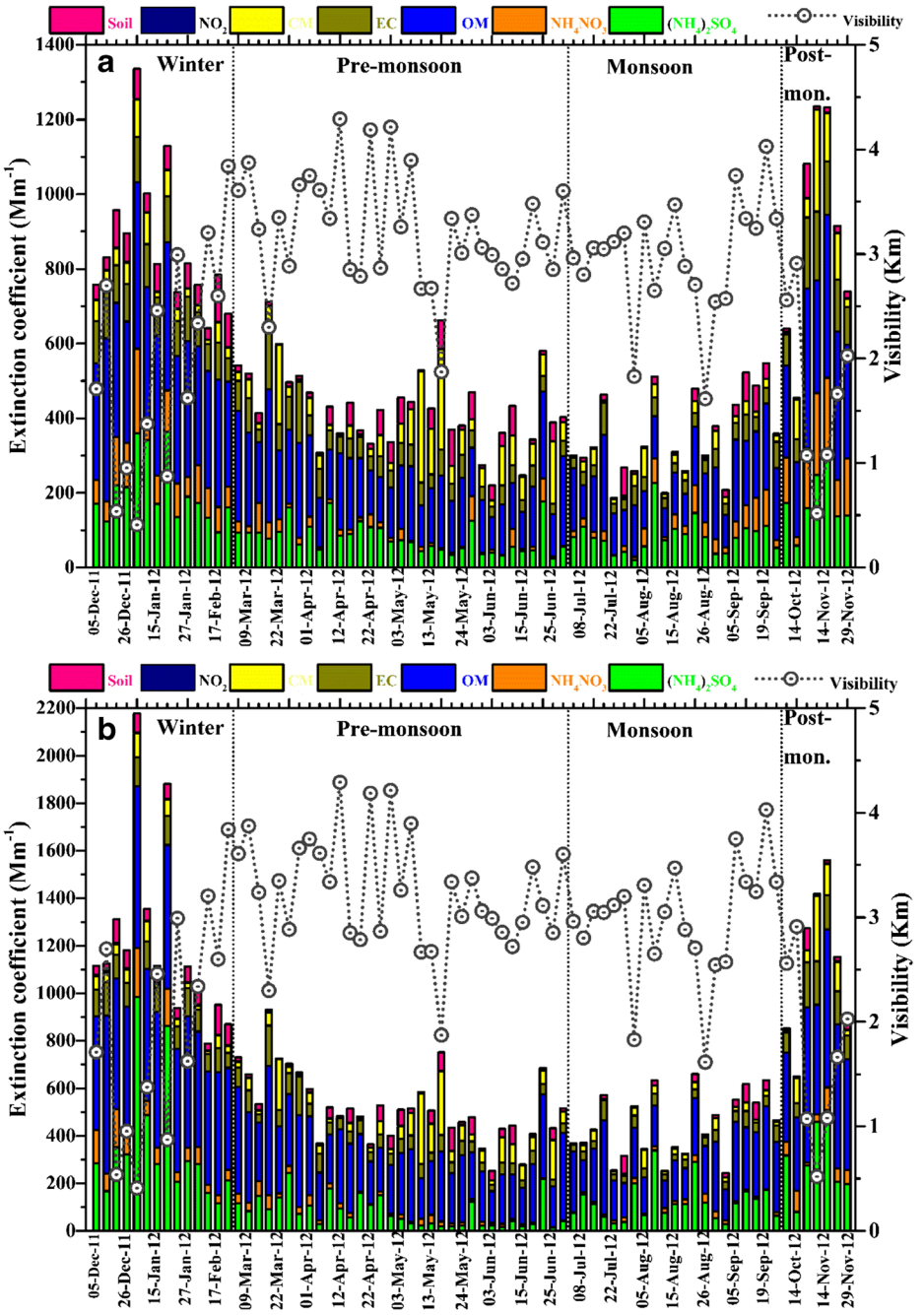

Fig. 7 Daily variability of the horizontal visibility and the cumulative contribution of each chemical component to the extinction coefficient obtained from the original IMPROVE (**a**) and from the revised IMPROVE (**b**) over Delhi from December 2011 to November 2012

those found for aerosol-pollution episodes (b_{ext} between ~0.6 and ~1.1 km^{-1} near the surface) over Kanpur (Kaskaoutis et al. 2013), indicating high pollution concentrations in Delhi during

the measurement period. High b_{ext} values of the same magnitude as those found in Delhi were estimated over the semi-arid urban site of Xi'an, China (Cao et al. 2012). The b_{ext} values exhibited an annual mean of 1102 ± 1020 Mm^{-1}, ranging from 711 ± 499 Mm^{-1} in spring (MAM) to 1607 ± 1361 Mm^{-1} in winter (Dec, Jan., and mid-Feb). Furthermore, seasonal-mean b_{ext} values from 193 ± 95 in spring to 319 ± 207 in autumn were estimated in rural Guangzhou, southern China (Chen et al. 2016). Seasonally-changing meteorological conditions, rainy washout, changes in mixing-layer height and boundary-layer dynamics, variations in emission rates and influence of long-range transported plumes of biomass smoke and/or desert dust are factors that result in the large daily and seasonal variation in b_{ext} (Hÿvarinen et al. 2011).

The daily b_{ext} estimations (Fig. 7a, b), as well as the seasonal means computed from the revised IMPROVE algorithm, are 22 % higher on an annual basis than those computed with the original IMPROVE algorithm. Figure 8 shows the correlation between the b_{ext} values computed from the original and the revised IMPROVE algorithms. A high correlation of $R^2 = 0.95$ is observed between the two sets of b_{ext} values showing very little scatter but a significant departure from the x = y line, especially for the larger b_{ext} values. The results show that the estimations of the two algorithms are very similar under relative clean to moderately polluted environments, but under turbid atmospheres, the revised IMPROVE algorithm computes significantly larger b_{ext} values. This result shows the influence of different hygroscopic growth factor values and the split of AS, AN, and OM into small and large modes concludes to overestimation of the b_{ext} especially under turbid environments (Pitchford et al. 2007). Unfortunately, measured b_{ext} values are not available for the study period so it is not possible to assess the suitability of the two algorithm versions in representing the light extinction over Delhi.

The relative (%) contribution of the individual components to estimate b_{ext} on a seasonal basis is shown in Fig. 9a, b for the original and revised IMPROVE algorithms, respectively. As

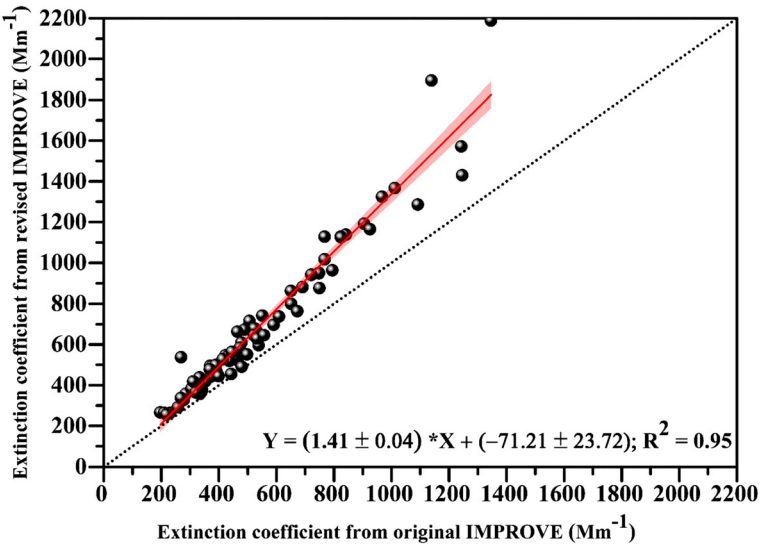

Fig. 8 Correlation between the b_{ext} values obtained from the original and revised versions of the IMPROVE algorithm over Dehi during December 2011–November 2012. The dotted line shows the linear regression and the pink area the limits of the linear regression at 95 % confidence level. The dotted line represents the 1–1

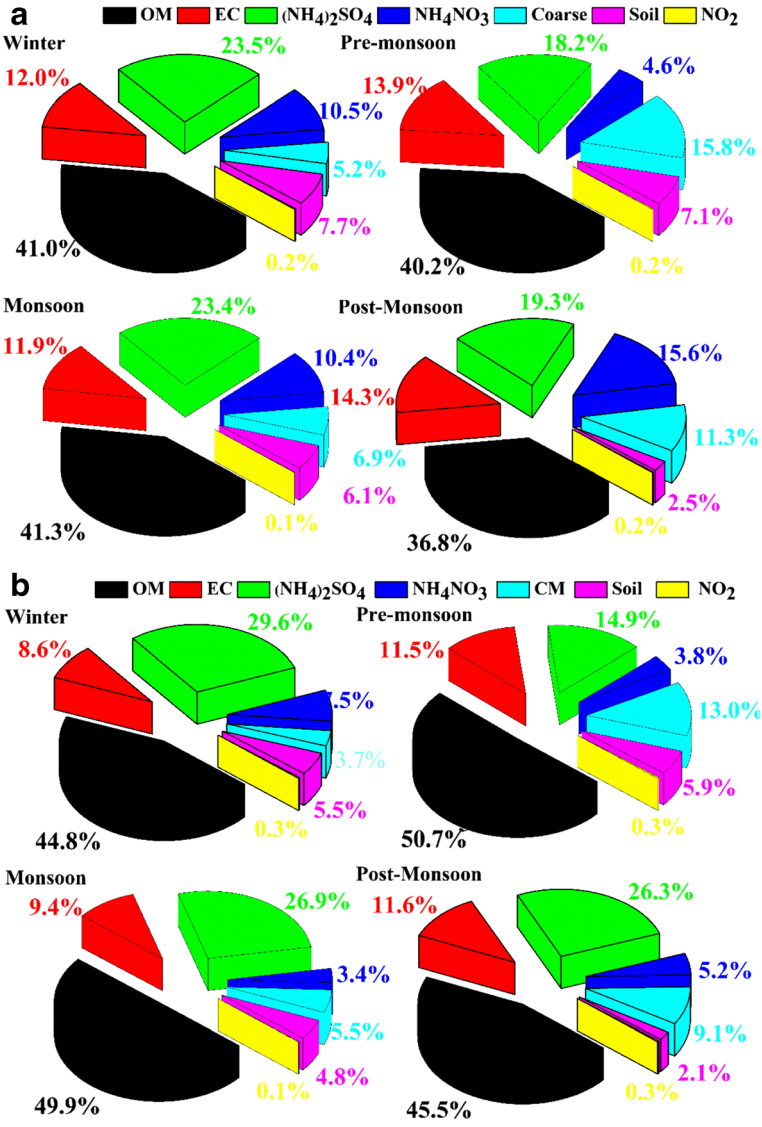

Fig. 9 Percentage (%) contribution of the chemical constituents to light extinction coefficient over Delhi for both the original (**a**) and the revised (b) IMPROVE algorithms on seasonal basis from during December 2011 – November 2012

far as the original IMPROVE is concerned, OM has the largest contribution to b_{ext} (~40 %, on an annual basis) followed by $(NH_4)_2SO_4$ (~21 %), EC (~13 %), coarse-mode particles (~10 %), NH_4NO_3 (~9 %) and soil (~6 %), while the contribution of NO_2 is negligible (0.1–0.2 %). Alternatively, the revised IMPROVE calculations showed that on annual basis, OM contributes to ~48 % to the b_{ext}, followed by $(NH_4)_2SO_4$ (~24 %), EC (~10 %), coarse mode (~8 %), NH_4NO_3 (~5 %) and soil (~5 %). The contribution of the chemical components to b_{ext} follows the same order for both IMPROVE versions, but the revised IMPROVE estimates a higher contribution from OM by ~8 %, with small (±2–3 %) differences in the other

components. This difference is because the measured OM belongs mostly in the large mode, which is associated with the higher coefficient (6.1) in the Eq. (3) compared to coefficient 4 in Eq. (1). This calculation results in much larger b_{ext} values for the OM estimated from the revised algorithm. However, the large contributions of EC remain despite its low fraction in the reconstructed (4.7–6.7 %) and measured (4.5 %) $PM_{2.5}$. This result highlights the significant impact of EC on solar-light extinction due to its strong absorbing capability (Bond et al. 2007, 2013).

Despite the much lower OM concentrations in pre-monsoon and monsoon (Table 1), the OM contribution to b_{ext} in these seasons is comparable or even higher to that of winter (Fig. 9a, b) underlying the significant role that CP play in atmospheric chemistry and radiation attenuation over Delhi throughout the year. In general, the contributions of EC and NH_4NO_3 to b_{ext} are higher during post-monsoon and winter from both algorithms due to the larger impact of agricultural and biofuel burning. Soil contributes from 2.5 % (post-monsoon) to 7.7 % (winter) for the original IMPROVE and from 2.1 % (post-monsoon) to 5.9 % (pre-monsoon) for the revised IMPROVE, exhibiting much lower contributions to b_{ext} compared to $PM_{2.5}$ (12.0–29.7 %) (Fig. 6). $(NH_4)_2SO_4$ contributes significantly (~15–30 %) all year long due to continuously high emissions of SO_2 and NH_3 over the urban environment (Behera and Sharma 2010b), while the revised IMPROVE algorithm estimates larger $(NH_4)_2SO_4$ contributions for the monsoon, post-monsoon, and winter and lower for pre-monsoon. Both algorithms agree that the highest contributions of coarse-mode particles to b_{ext} is in pre-monsoon (15.8 % and 13 %) due to much larger dust influence (Lodhi et al. 2013). The coarse mode contributions in winter are smaller (5.2 % and 3.7 %), suggesting that the vast majority of the particles are below 2.5 μm, similar to Komppula et al. (2012). The coarse-mode aerosol contribution to b_{ext} is also important during post-monsoon (11.3 % and 9.1 %), suggesting that the smoke particles may also be found in coarse mode after aging, condensation and coagulation processes during their transportation (Dumka et al. 2015).

A similar approach for estimation of b_{ext} via chemical analysis of $PM_{2.5}$ in China (Cao et al. 2012) revealed largest contribution (~40 %) of $(NH_4)_2SO_4$, followed by OM (~24 %), NH_4NO_3 (~23 %) and EC (~9 %), with minor contributions from soil dust (~3 %) and NO_2 (~1 %). The dominance of CP (OM: 39.3 % and EC: ~20 %) on b_{ext} during winter was also found at Pearl River Delta, China (Zhang et al. 2013b) followed by $(NH_4)_2SO_4$ (16 %), coarse mode (13 %) and NH_4NO_3 (11.8 %).

Light extinction is strongly linked with visibility impairment (Cao et al. 2012). The recorded daily horizontal visibility in Delhi is plotted against the estimated b_{ext} values from both algorithm versions in Fig. 10. Strong negative correlations ($P < 0.05$) with visibility, associated with 51 % and 54 % of the variance (R^2), are calculated for the original and revised IMPROVE estimates of b_{ext}, indicating a direct impact of aerosol mass concentration on visibility degradation, as expected. In both cases, the scatter of the data points increases for the lower b_{ext} values, while for visibility values below 1.5 km, which correspond to very turbid atmospheres (dust storms or heavy haze/fog conditions), the b_{ext} estimates from the revised algorithm are significantly higher. However, changes in RH affect b_{ext} (see Eqs. 1 and 3) and its relationship with visibility due to the formation of low-level fog during winter and decreasing of visibility due to humid atmospheres during monsoon, resulting in weakening the correlation between b_{ext} and horizontal visibility. Furthermore, the visibility values were classified into five groups (1-km interval from 0 to 5 km), that are compared to the b_{ext} values estimated via both IMPROVE algorithms (Fig. 11a, b). During the study period, the mean visibility was found to be 2.8 ± 0.9 km, varying from 1.7 ± 0.80 km (post-monsoon) to 3.2 ± 0.5 km (pre-monsoon). Decreased visibility is associated with an increase in b_{ext} from 404 ± 89 Mm^{-1} for visibility 4–5 km to 500 ± 191 Mm^{-1} (vis =2–3 km) and 1120 ± 165 Mm^{-1}

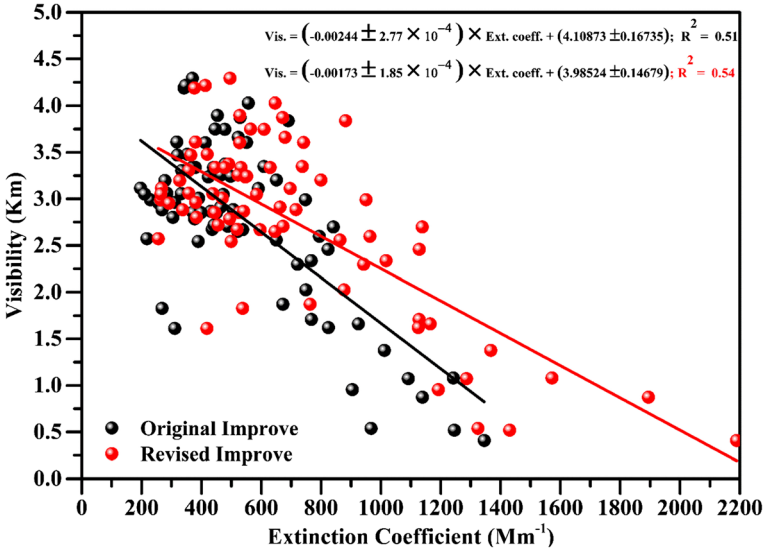

Fig. 10 Correlation between the visibility and b_{ext} values estimated from the original and the revised IMPROVE algorithms over Delhi during December 2011–November 2012

(vis < 1 km), according to the original IMPROVE estimations. The revised IMPROVE increases further the b_{ext} for the lowest visibility ranges, up to ~1600 Mm^{-1} for visibility <1 km. This strong negative correlation supports the use of the current methodology for the estimations of b_{ext} across Delhi. Similar atmospheric conditions of haze/fog formation are usually observed over polluted sites in China, where the high concentrations of secondary inorganic constituents (SO_4^{2-} and NO_3^-) were found to have a major impact on visibility degradation (Cao et al. 2012).

Figure 12 examines the influence of anthropogenic [OM + EC + NH_4NO_3 + $(NH_4)_2SO_4$] and natural aerosols (soil + coarse mode) on b_{ext} estimates from both algorithms. Strong relationships (R^2 = 0.94 and R^2 = 0.97) are found between b_{ext} and anthropogenic components (Fig. 12a, c), suggesting that the urban/anthropogenic emissions play the major role in light extinction and visibility impairment in Delhi. The natural-origin particles also contribute to b_{ext}, but both the correlations are associated with large scatter (Fig. 12b, d) indicating that their role in the extinction of solar light is much lesser than that of anthropogenic aerosols. When the concentrations of the natural component are below 100 μg m^{-3}, the relationships with b_{ext} are rather neutral. However, it should be noted that the assumption that the soil and coarse-mode particles are exclusively of natural origin is a first approximation since anthropogenic activities and farming practices also emit soil particles as well as the re-suspension of soil dust by road traffic. In contrast, F^- may also indicate non-soil particles (Kumar et al. 2010), while a part of the OM, which is considered as anthropogenic in Figs. 12a, c may be derived from biogenic volatile organic compounds (VOC's). However, these fractions are very difficult to quantify with detailed organic speciation and, therefore, the classification of anthropogenic and natural particles is subjected to bias.

4 Conclusions

Chemical analysis for carbonaceous constituents (OC, EC) and ionic species (SO_4^{2-}, NO_3^-, NH_4^+ and F^-) was performed on 75 $PM_{2.5}$ samples collected in Delhi from December 2011 to

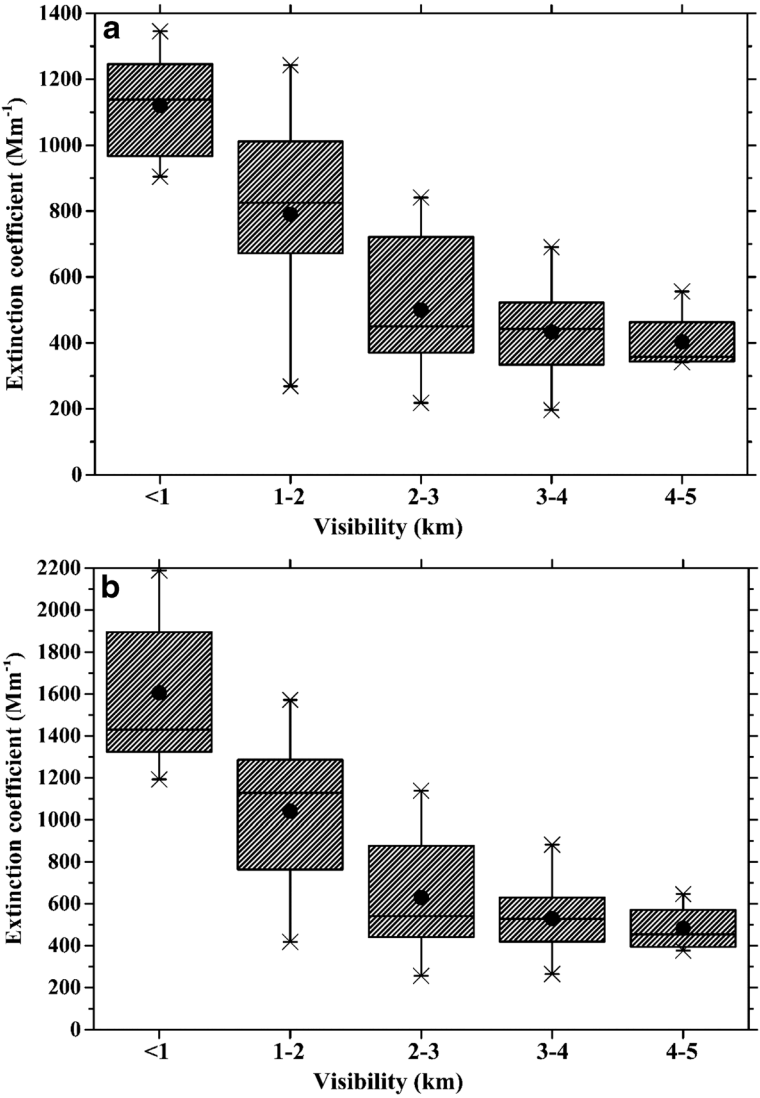

Fig. 11 Box and whisker plots (as in Fig. 4) of the extinction coefficient for 5 groups of horizontal visibility for both original IMPROVE (**a**) and revised IMPROVE (**b**) estimates

November 2012. Additional measurements of PM_{10} mass concentrations, meteorological parameters, and horizontal visibility were made. Analyses focused on examining the seasonality of the particulate chemical components and their contribution to the extinction coefficient (b_{ext}) and visibility degradation. The annual-averaged $PM_{2.5}$ mass concentration was 153.6 ± 59.8 μg m^{-3}, from which the OC (33.5 ± 15.9 μg m^{-3}, 22 % of $PM_{2.5}$) and the ionic species (~34.9 ± 21.5 μg m^{-3}, ~23 %) hold the largest fractions, followed by EC (6.9 ± 3.9 μg m^{-3}, ~5 %). The $PM_{2.5}$, OC and EC concentrations exhibited significant daily and seasonal variations peaking during post-monsoon and winter. The average OC/EC of 5.18 ± 1.47 (range from 2.45 to 9.26) indicated various types of carbonaceous aerosol emission sources (combustion of diesel, gasoline, coal, burning of biofuels/biomass). Primary and

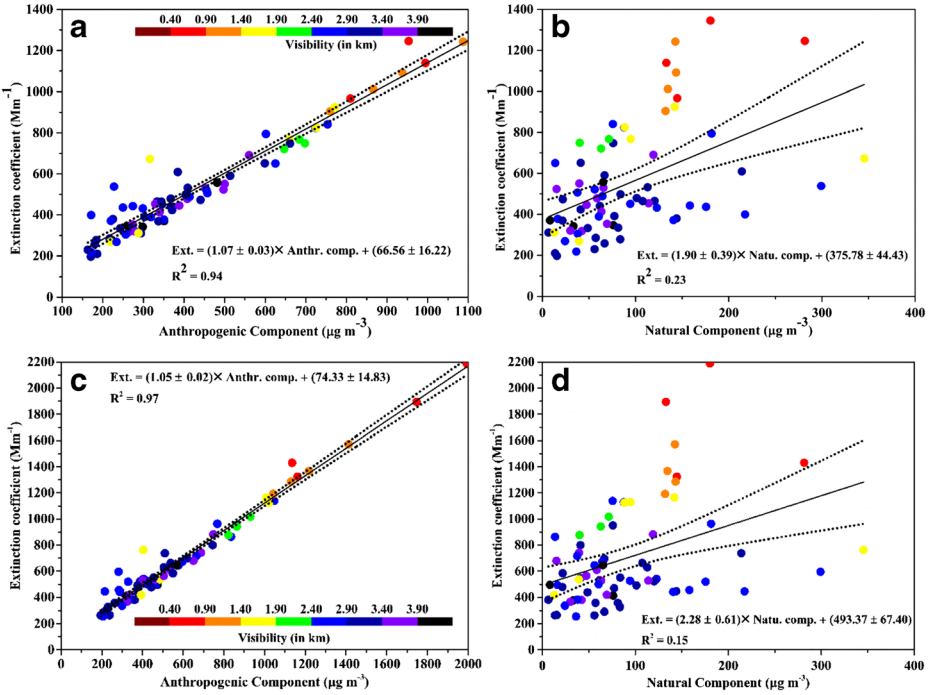

Fig. 12 Correlation between anthropogenic [OM + EC + NH_4NO_3 + $(NH_4)_2SO_4$] (**a**, **c**) and natural (soil + coarse mode) (**b**, **d**) concentrations with extinction coefficient as function of visibility for the 75 $PM_{2.5}$ samples in Delhi during December 2011–November 2012. The dotted lines show the lower and upper 95 % confidence levels of the linear regressions. The upper graphs (**a**, **b**) are for original-IMPROVE b_{ext} retrievals and the lower ones (**c**, **d**) for b_{ext} retrievals from the revised IMPROVE

secondary OC were found to be of the same magnitude (17.0 and 16.7 μg m^{-3}, respectively), exhibiting significant seasonal variability with larger concentrations in post-monsoon and winter. Secondary organic aerosol formation accounted for ~18 % of $PM_{2.5}$, revealing a mean concentration of 26.7 ± 14.8 μg m^{-3}. The highest concentrations of SO_4^{2-} (39.4 μg m^{-3}) and NO_3^- (29.6 μg m^{-3}) were observed in November 2012, associated with major agricultural biomass burning in northwestern India. Estimates of b_{ext} were performed via $PM_{2.5}$ chemical analysis using the original and the revised IMPROVE algorithms. Very large daily variability was found between the estimated b_{ext} values, which on the seasonal basis were found to maximize during post-monsoon and winter and to be strongly related (r = −0.72) with visibility impairment over Delhi. The percentage contributions of the chemical species to b_{ext} were seasonally dependent, following the order of OM (~40 %, 48 %), $(NH_4)_2SO_4$ (~21 %, 24 %), EC (~13 %, 10 %), coarse-mode aerosols (~10 %, 8 %), NH_4NO_3 (~9 %, 5 %), soil (~6 %, 5 %) and NO_2 (~0.2 %, 0.3 %), on annual basis for the original and the revised IMPROVE algorithms. The revised IMPROVE estimated significantly higher values of the b_{ext} for more turbid atmospheres and for visibility ranges below 1 km compared to the original algorithm; however, the b_{ext} values from both algorithms were highly correlated (R^2 = 0.95). Future works exploring the suitability of the IMPROVE algorithms in simulating the measured b_{ext} using the larger dataset of $PM_{2.5}$ samples will contribute significantly in monitoring the pollution/haze episodes over Delhi and helping the policy makers for mitigating efforts.

The current work is the first attempt to estimate the b_{ext} for the Delhi polluted atmosphere using chemical analysis of $PM_{2.5}$ samples using the original and revised versions of the IMPROVE algorithm. In general, the estimated b_{ext} values follow the seasonality revealed from previous studies over Delhi and surroundings using in-situ (Nephelometer/Aethalometer) measurements and/or LIDAR profiles, giving support to the current estimates, especially due to an absence of validation procedure since measured b_{ext} is not available. Comparison with measurements at 21 sites in the USA showed that the original algorithm underestimated the highest b_{ext} values and overestimated the lowest ones. The revised algorithm reduced the under-prediction in b_{ext} under severe haze conditions and the over-prediction during low-haze periods compared with the original algorithm (Pitchford et al. 2007). Future work using a larger and more complete chemically characterized dataset of $PM_{2.5}$ samples for more representative analysis regarding the seasonality of $PM_{2.5}$, carbonaceous aerosols, and inorganic species, along with validation of the b_{ext} estimations against ground-based measurements will allow further use of chemical compositions for estimating extinction coefficients and visibility degradation across Delhi.

Acknowledgments The authors thank the Director, IITM Pune and Ministry of Earth Science, Government of India for their constant encouragement and support of the research work. The authors also gratefully acknowledge the NOAA Air Resources Laboratory (ARL) for the provision of the HYSPLIT transport and dispersion model and/or READY website (http://www.ready.noaa.gov) used in this study. UCD and DGK greatly appreciate the fruitful communications and comments provided by Prof. Nikos Mihalopoulos. Authors would like to thanks the editor in Chief Prof. E. Atlas and anonymous reviewers for their constructive comments and suggestions which helped us to improve the manuscript.

References

Andreae, M., Gelencsér, A.: Black carbon or brown carbon? The nature of light-absorbing carbonaceous aerosols. Atmos Chem Phys. **6**, 3131–3148 (2006)

Badarinath, K.V.S., Kharol, S.K., Krishna Prasad, V., Reddi, E.U.B., Kambezidis, H.D., Kaskaoutis, D.G.: Influence of natural and anthropogenic activities on UV index variations–a study over tropical urban region using ground based observations and satellite data. J Atmos Chem. **59**, 219–236 (2008)

Behera, S.N., Sharma, M.: Investigating the potential role of ammonia in ion chemistry of fine particulate matter formation for an urban environment. Sci Total Environ. **408**, 3569–3575 (2010a)

Behera, S.N., Sharma, M.: Reconstructing primary and secondary components of $PM_{2.5}$ compositions for an urban atmosphere. Aer SciTechn. **44**, 983–992 (2010b)

Birch, M.E., Cary, R.A.: Elemental carbon-based method for monitoring occupational exposures to particulate diesel exhaust. Aerosp Sci Technol. **25**, 221–241 (1986)

Bisht, D.S., Dumka, U.C., Kaskaoutis, D.G., Pipal, A.S., Srivastava, A.K., Soni, V.K., Attri, S.D., Sateesh, M., Tiwari, S.: Carbonaceous aerosols and pollutants over Delhi urban environment: temporal evolution, source apportionment and radiative forcing. Sci Total Environ. **521–522**, 431–445 (2015)

Bond, T.C., Bhardwaj, E., Dong, R., Jogani, R., Jung, S., Roden, C., Streets, D.G., Trautmann, N.M.: Historical emissions of black and organic carbon aerosol from energy related combustion, 1850–2000. Glob Biogeochem Cycles. **21**, GB2018 (2007). doi:10.1029/2006GB002840

Bond, T.C., Doherty, S.J., Fahey, D.W., Forster, P.M., Berntsen, T., DeAngelo, B.J., Flanner, M.G., Ghan, S., Karcher, B., Koch, D., Kinne, S., Kondo, Y., Quinn, P.K., Sarofim, M.C., Schultz, M.G., Schulz, M., Venkataraman, C., Zhang, H., Zhang, S., Bellouin, N., Guttikunda, S.K., Hopke, P.K., Jacobson, M.Z., Kaiser, J.W., Klimont, Z., Lohmann, U., Schwarz, J.P., Shindell, D., Storelvmo, T., Warren, S.G., Zender, C.S.: Bounding the role of black carbon in the climate system: A scientific assessment. J Geophys Res. **118**, 5380–5552 (2013)

Bougiatioti, A., Zarmpas, P., Koulouri, E., Antoniou, M., Theodosi, C., Kouvarakis, G., Saarikoski, S., Mäkelä, T., Hillamo, R., Mihalopoulos, N.: Organic, elemental and water-soluble organic carbon in size segregated aerosols, in the marine boundary layer of the eastern Mediterranean. Atmos Environ. **64**, 251–262 (2013)

Cao, J., Wang, Q.-Y., Chow, J.C., Watson, J.G., Tie, X.-X., Shen, Z.-X., Wang, P., An, Z.-S.: Impacts of aerosol compositions on visibility impairment in Xi'an. China. Atmos. Environ. 59, 559–566, (2012).

Castro, L.M., Pio, C.A., Harrison, R.M., Smith, D.J.T.: Carbonaceous aerosol in urban and rural European atmospheres: estimation of secondary organic carbon concentrations. Atmos Environ. **33**, 2771–2781 (1999)

Chen, Y., Zhi, G., Feng, Y., Fu, J., Feng, J., Sheng, G., Simoneit, B.R.T.: Measurements of emission factors for primary carbonaceous particles from residential raw-coal combustion in China. Geophys Res Lett. **33**, (2006). doi:10.1029/2006GL026966

Chen, X., Lai, S., Gao, Y., Zhang, Y., Zhao, Y., Chen, D., Zheng, J., Zhong, L., Lee, S.-C., Chen, B.: Reconstructed light extinction coefficients of fine particulate matter in rural Guangzhou. Southern China Aer Air Qual Res. **16**, 1981–1990 (2016)

Chow, J.C., Watson, J.G., Chen, L.-W.A., Arnott, W.P., Moosmüller, H., Fung, K.K.: Equivalence of elemental carbon by thermal/optical reflectance and transmittance with different temperature protocols. Environ Sci Technol. **38**, 4414–4422 (2004)

Decesari, S., Facchini, M.C., Fuzzi, S., Tagliavini, E.: Characterization of water-soluble organic compounds in atmospheric aerosol: a new approach. J Geophys Res. **105**, 1481–1489 (2000)

Dey, S., Girolamo, L.D., Van Donkelaar, A., Tripathi, S.N., Gupta, T., Mohan, M.: Variability of outdoor fine particulate ($PM_{2.5}$) concentration in the Indian Subcontinent: A remote sensing approach. Remote Sens Environ. **127**, 153–161 (2012)

Draxler, R.R., Rolph, G.D., HYSPLIT (HYbrid Single-Particle Lagrangian Integrated Trajectory) Model access via NOAA ARL READY Website (http://ready.arl.noaa.gov/HYSPLIT.php). NOAA Air Resources Laboratory, Silver Spring, MD (2016)

Dumka, U.C., Kaskaoutis, D.G., Srivastava, M.K., Devara, P.C.S.: Scattering and absorption properties of near-surface aerosol over Gangetic–Himalayan region: the role of boundary-layer dynamics and long-range transport. Atmos Chem Phys. **15**, 1555–1572 (2015)

Feng, Y., Chen, Y., Guo, H., Zhi, G., Xiong, S., Li, J., Sheng, G., Fu, J.: Characteristics of organic carbon in $PM_{2.5}$ samples in Shanghai, China. Atmos Res. **92**, 434–442 (2009)

Foyo-Moreno, I., Alados, I., Antón, M., Fernández-Gálvez, J., Cazorla, A., Alados-Arboledas, L.: Estimating aerosol characteristics from solar irradiance measurements at an urban location in southeastern Spain. J Geophys Res. **119**, 1845–1859 (2014). doi:10.1002/2013JD020599

Ganguly, D., Rasch, P.J., Wang, H., Yoon, J.-H.: Climate response of the south Asian monsoon system to anthropogenic aerosols. J Geophys Res. **117**, D13209 (2012). doi:10.1029/2012JD017508

Gautam, R., Hsu, N.C., Kafatos, M., Tsay, S.–C.: Influences of winter haze on fog/low cloud over the Indo-Gangetic plains. J Geophys Res. **112**, D05207 (2007). doi:10.1029/2005JD007036

Guinot, B., Cachier, H., Oikonomou, K.: Geochemical perspectives from a new aerosol chemical mass closure. Atmos Chem Phys. **7**, 1657–1670 (2007)

Guttikunda, S.K., Calori, G.: A GIS based emissions inventory at 1 km × 1 km spatial resolution for air pollution analysis in Delhi. India Atmos Environ. **67**, 101–111 (2013)

Hoyle, C.R., Boy, M., Donahue, N.M., Fry, J.L., Glasius, M., Guenther, A., et al.: A review of the anthropogenic influence on biogenic secondary organic aerosol. Atmos Chem Phys. **11**, 321–343 (2011)

Huang, L.-K., Wang, G.-Z., Wang, K.: Physicochemical characteristics and long-range transportation of atmospheric particulates during a dust storm episode in Harbin. China Zhongguo Huanjing Kexue/China Environ Sci. **34**, 1920–1926 (2014)

Hÿvarinen, A.-P., Raatikainen, T., Komppula, M., Mielonen, T., Sundström, A.-M., Brus, D., Panwar, T.S., Hooda, R.K., Sharma, V.P., de Leeuw, G., Lihavainen, H.: Effect of the summer monsoon on aerosols at two measurement stations in northern India – part 2: physical and optical properties. Atmos Chem Phys. **11**, 8283–8294 (2011)

IMPROVE: "Spatial and Seasonal Patterns and Temporal Variability of Haze and Its Constituents in the United States," Report V, ISSN 0737–5352-87, available from http://vista.cira.colostate.edu/improve/publications/reports/2011/PDF/IMPROVE_V_FullReport.pdf (2011)

Jimenez, J.L., Canagaratna, M.R., Donahue, N.M., Prevot, A.S.H., et al.: 2009. Evolution of organic aerosols in the atmosphere. Science. **326**, 1525–1529 (2009)

Kamani, H., Ashrafi, S.D., Isazadeh, S., Jaafari, J., Hoseini, M., Mostafapour, F.K., Bazrafshan, E., Nazmara, S., Mahvi, A.H.: Heavy metal contamination in street dusts with various land uses in Zahedan. Iran Bull Environ Contam Toxicol. **94**(3), 382–386 (2015)

Kaskaoutis, D.G., Sinha, P.R., Vinoj, V., Kosmopoulos, P.G., Tripathi, S.N., Misra, A., Sharma, M., Singh, R.P.: Aerosol properties and radiative forcing over Kanpur during severe aerosol loading conditions. Atmos Environ. **79**, 7–19 (2013)

Kaskaoutis, D.G., Kumar, S., Sharma, D., Singh, R.P., Kharol, S.K., Sharma, M., Singh, A.K., Singh, S., Singh, A., Singh, D.: Effects of crop residue burning on aerosol properties, plume characteristics and long-range transport over northern India. J Geophys Res. **119**, 5424–5444 (2014). doi:10.1002/2013JD021357

Khalil, S.A., Shaffie, A.M.: Attenuation of the solar energy by aerosol particles: a review and case study. Renew Sust Energ Rev. **54**, 363–375 (2016)

Komppula, M., Mielonen, T., Arola, A., Korhonen, K., Lihavainen, H., Hyvarinen, A.-P., Baars, H., Engelmann, R., Althausen, D., Ansmann, A., Müller, D., Panwar, T.S., Hooda, R.K., Sharma, V.P., Kerminen, V.-M., Lehtinen, K.E.J., Viisanen, Y.: One year of Raman-lidar measurements in Gual Pahari EUCAARI site close to New Delhi in India: seasonal characteristics of the aerosol vertical structure. Atmos Chem Phys. **12**, 4513–4524 (2012)

Kumar, A., Sarin, M.M., Srinivas, B.: Aerosol iron solubility over bay of Bengal: role of anthropogenic sources and chemical processing. Mar Chem. **121**, 167–175 (2010)

Kumar, R., Naja, M., Satheesh, S.K., Ojha, N., Joshi, H., Sarangi, T., Pant, P., Dumka, U.C., Hegde, P., Venkataramani, S.: Influences of the springtime northern Indian biomass burning over the central Himalayas. J Geophys Res. **116**, D19302 (2011). doi:10.1029/2010JD015509

Li, H., Feng, J., Sheng, G., Lü, S., Fu, J., Peng, P., Ren, M.: The PCDD/F and PBDD/F pollution in the ambient atmosphere of shanghai. China Chemosphere. **70**, 576–583 (2008)

Lodhi, N.K., Beegum, S.N., Singh, S., Kumar, K.: Aerosol climatology at Delhi in the western indo-Gangetic plain: microphysics, long-term trends, and source strengths. J Geophys Res. **118**, 1361–1375 (2013). doi:10.1002/jgrd.50165

Lu, Z., Zhang, Q., Streets, D.G.: Sulfur dioxide and primary carbonaceous aerosol emissions in China and India, 1996–2010. Atmos Chem Phys. **11**, 9839–9864 (2011)

Malm, W.C., Day, D.E.: Estimates of aerosol species scattering characteristics as a function of relative humidity. Atmos Environ. **35**, 2845–2860 (2001)

Mantas, E., Remoundaki, E., Halari, I., Kassomenos, P., Theodosi, C., Hatzikioseyian, A., Mihalopoulos, N.: Mass closure and source apportionment of $PM_{2.5}$ by Positive Matrix Factorization analysis in urban Mediterranean environment. Atmos Environ. **94**, 154–163 (2014)

Misra, A., Tripathi, S.N., Kaul, D., Welton, E.: Study of MPLNET derived aerosol climatology over Kanpur, India, and validation of CALIPSO level 2 version 3 backscatter and extinction products. J Atmos Ocean Technol. **29**, 1285–1294 (2012)

Nair, V.S., Solmon, F., Giorgi, F., et al.: Simulation of south Asian aerosols for regional climate studies. J Geophys Res. **117**, D04209 (2012). doi:10.1029/2011JD016711

Novakov, T., Menon, S., Kirchstetter, T.W., Koch, D., Hansen, J.E.: Aerosol organic carbon to black carbon ratios: analysis of published data and implications for climate forcing. J Geophys Res. **110**, D21205 (2005). doi:10.1029/2005JD005977

Panda, S., Sharma, S.K., Mhapatra, P.S., Panda, U., Rath, S., Mhapatra, M., Mandal, T.K., Das, T.: Organic and elemental carbon variation in PM2.5 over megacity Delhi and Bhubaneswar, a semi-urban coastal site in India. Nat Hazards. **80**, 1709–1728 (2016)

Pandey, P., Khan, A.H., Verma, A.K., Singh, K.A., Mathur, N., Kisku, G.C., Barman, S.C.: Seasonal Trends of $PM_{2.5}$ and PM_{10} in Ambient Air and Their Correlation in Ambient Air of Lucknow City, India. Bull Environ ContamToxicol. **88**(2), 265–270 (2012)

Paraskevopoulou, D., Liakakou, E., Gerasopoulos, E., Theodosi, C., Mihalopoulos, N.: Long-term characterization of organic and elemental carbon in the $PM_{2.5}$ fraction: the case of Athens, Greece. Atmos Chem Phys. **14**, 13313–13325 (2014). doi:10.5194/acp-14-13313-2014

Pateraki, S., Asimakopoulos, D.N., Bougiatioti, A., Maggos, T., Vasilakos, C., Mihalopoulos, N.: Assessment of $PM_{2.5}$ and PM_1 chemical profile in a multiple-impacted Mediterranean urban area: origin, sources and meteorological dependence. Sci Total Environ. **479–480**, 210–220 (2014)

Pio, C., Cerqueira, M., Harrison, R.M., Nunes, T., Mirante, F., Alves, C., Oliveira, C., de la Campa A, S., Artíñano, B., Matos, M.: OC/EC ratio observations in Europe: Re-thinking the approach for apportionment between primary and secondary organic carbon. Atmos Environ. **45**, 6121–6132 (2011)

Pipal, A.S., Kulshrestha, A., Taneja, A.: Characterization and morphological analysis of airborne $PM_{2.5}$ and PM_{10} in Agra located in North Central part of India. Atmos Environ. **45**, 3621–3630 (2011)

Pitchford, M.L., Malm, W.C., Schichtel, B.A., Kumar, N.K., Lowenthal, D.H., Hand, J.L.: Revised algorithm for estimating light extinction from IMPROVE particle speciation data. J Air Waste Manage Assoc. **57**, 1326–1336 (2007)

Putaud, J.-P., Van Dingenen, R., Alastuey, A., Bauer, H., Birmili, W., et al.: A European aerosol phenomenology - 3: physical and chemical characteristics of particulate matter from 60 rural, urban, and kerbside sites across Europe. Atmos Environ. **44**, 1308–1320 (2010)

Ram, K., Sarin, M.M.: Day-night variability of EC, OC, WSOC and inorganic ions in urban environment of Indo-Gangetic Plain: Implications to secondary aerosol formation. Atmos Environ. **45**, 460–468 (2011)

Ram, K., Sarin, M.M.: Atmospheric carbonaceous aerosols from indo-Gangetic plain and central Himalaya: impact of anthropogenic sources. J Environ Manag. **148**, 153–163 (2015)

Ram, K., Sarin, M.M., Hegde, P.: Atmospheric abundances of primary and secondary carbonaceous species at two high-altitude sites in India: sources and temporal variability. Atmos Environ. **4**, 6785–6796 (2008)
Ram, K., Sarin, M.M., Tripathi, S.N.: A 1 year record of carbonaceous aerosols from an urban site in the indo-Gangetic plain: characterization, sources, and temporal variability. J Geophys Res. **11**, D24313 (2010a). doi:10.1029/2010JD014188
Ram, K., M.M., S., Hegde, P.: Long-term record of aerosol optical properties and chemical composition from a high-altitude site (Manora Peak) in Central Himalaya. Atmos Chem Phys. **10**, 11791–11803 (2010b)
Ram, K., Sarin, M.M., Tripathi, S.N.: Temporal trends in atmospheric $PM_{2.5}$, PM_{10}, elemental carbon, organic carbon, water-soluble organic carbon, and optical properties: Impact of biomass burning emissions in the Indo-Gangetic Plain. Environ. Sci. Technol. **46**, 686–695 (2012)
Rastogi, N., Singh, A., Singh, D., Sarin, M.M.: Chemical characteristics of $PM_{2.5}$ at a source region of biomassburning emissions: Evidence for secondary aerosol formation. Environ Pollut. **184**, 563–569 (2014)
Reddington, C.L., Butt, E.W., Ridley, D.A., Artaxo, P., Morgan, W.T., Coe, H., Spracklen, D.V.: Air quality and human health improvements from reductions in deforestation-related fire in Brazil. Nat Geosci. **8**, 768–773 (2015). doi:10.1038/NGEO2535
Rengarajan, R., Sarin, M.M., Sudheer, A.K.: Carbonaceous and inorganic species in atmospheric aerosols during wintertime over urban and high-altitude sites in North India. J Geophys Res. **112**, D21307 (2007). doi:10.1029/2006JD008150
Robinson, A.L., Donahue, N.M., Shrivastava, M.K., Weitkamp, E.A., Sage, A.M., Grieshop, A.P., Lane, T.E., Pierce, J.R., Pandis, S.N.: Rethinking organic aerosols: Semivolatile emissions and photochemical aging. Science. **315**, 1259–1262 (2007)
Saxena, M., Sharma, S.K., Mandal, T.K., Singh, S., Saud, T.: Source apportionment of particulates by receptor models over bay of Bengal during ICARB campaign. Atmos Poll Res. **5**, 729–740 (2014)
Sharma, M., Maloo, S.: Assessment of ambient air PM_{10} and $PM_{2.5}$ and characterization of PM_{10} in the city of Kanpur, India. Atmos Environ. **39**, 6015–6026 (2005)
Sharma, S.K., Mandal, T.K., Saxena, M., Rashmi, R., Sharma, A., Datta, A., Saud, T.: Variation of OC, EC, WSIC and trace metals of PM_{10} in Delhi. India J Atmos Solar-Terr Phys. **113**, 10–22 (2014)
Sharma, S.K., Sharma, A., Saxena, M., Choudhary, N., Masiwal, R., Mandal, T.K., Sharma, C.: Chemical characterization and source apportionment of aerosol at an urban area of Central Delhi. India Atmos Pollut Res. **7**, 110–121 (2016)
Shen, G., Xue, M., Yuan, S., Zhang, J., Zhao, Q., Li, B., Wu, H.: Ding, a: chemical compositions and reconstructed light extinction coefficients of particulate matter in a mega-city in the western Yangtze River Delta. China Atmos Environ. **83**, 14–20 (2014)
Singh, A., Rajput, P., Sharma, D., Sarin, M.M., Singh, D.: Black carbon and elemental carbon from postharvest agricultural-waste burning emissions in the Indo-Gangetic Plain. Adv Meteorol. ID 179301 (2014). doi:10.1155/2014/179301
Smith, D.J.T., Harrison, R.M., Luhana, L., Pio, C.A., Castro, L.M., Tariq, M.N., Harat, S., Quraishi, T.: Concentration of particulate airborne poly-aromatic hydrocarbons and metals collected in Lahore. Pakistan Atmos Environ. **30**, 4031–4040 (2007)
Srinivas, B., Sarin, M.M.: $PM_{2.5}$, EC and OC in atmospheric outflow from the Indo-Gangetic Plain: Temporal variability and aerosol organic carbon-to-organic mass conversion factor. Sci Total Environ. **487**, 196–205 (2014)
Srivastava, A.K., Singh, S., Tiwari, S., Kanawade, V.P., Bisht, D.S.: Variationbetween near-surface and columnar aerosol characteristics during winters andsummers at a station in the Indo-Gangetic Basin. J Atmos Solar-Terr Phys. **77**, 57–66 (2012)
Streets, D.G., Bond, T.C., Lee, T., Jang, C.: On the future of carbonaceous aerosol emissions. J Geophys Res. **109**, D24212 (2004). doi:10.1029/2004JD004902
Tao, J., Zhang, L., Ho, K., Zheng, R., Lin, Z., Zhang, Z., Lin, M., Cao, J., Liu, S., Wang, G.: Impact of $PM_{2.5}$ chemical compositions on aerosol light scattering in Guangzhoue the largest megacity in South China. Atmos Res. **135–136**, 48–58 (2014)
Taylor, S.R., McLennan, S.M.: The continental crust: its composition and evolution, p. 312p. Blackwell Scientific Publication, Carlton (1985)
Tiwari, S., Srivastava, A.K., Bisht, D.S., Bano, T., Singh, S., Behura, S., Srivastava, M.K., Chate, D.M., Padmanabhamurty, B.: Black Carbon and Chemical characteristics of PM_{10} and $PM_{2.5}$ at an urban site of North India. Intern J Atmos Chem. **62**, 3193–3209 (2009)
Tiwari, S., Chate, D.M., Srivastava, M.K., Safai, P.D., Srivastava, A.K., Bisht, D.S., Padmanabhamurty, B.: Statistical evaluation of PM_{10} and distribution of PM_1, $PM_{2.5}$, and PM_{10} in ambient air due to extreme fireworks episodes (Diwali festivals) in megacity Delhi. Nat Hazards. **61**, 521–531 (2012)
Tiwari, S., Srivastava, A.K., Bisht, D.S., Safai, P.D.: Assessment of carbonaceousaerosol over Delhi in the Indo-Gangetic Basin: characterization, sources andtemporal variability. Nat Hazards. **65**, 1745–1764 (2013a)

Tiwari, S., Srivastava, A.K., Bisht, D.S., Parmita, P., Srivastava, M.K., Attri, S.D.: Diurnal and seasonal variations of black carbon and $PM_{2.5}$ over New Delhi, India: Influence of meteorology. Atmos Res. **125–126**, 50–62 (2013b)

Tiwari, S., Bisht, D.S., Srivastava, A.K., Pipal, A.S., Taneja, A., Srivastava, M.K., Attri, S.D.: Variability in atmospheric particulates and meteorological effects on its mass concentrations over Delhi. India Atmos Res. **145-146**, 45–56 (2014)

Tiwari, S., Pipal, A.S., Hopke, P.K., Bisht, D.S., Srivastava, A.K., Tiwari, S., Saxena, P.N., Khan, A.H., Pervez, S.: Study of the carbonaceous aerosol and morphological analysis of fine particles along with their mixing state in Delhi, India: a case study. Environ Sci Pollut Res. **22**, 10744 (2015). doi:10.1007/s11356-015-4272-6

Tiwari, S., Dumka, U.C., Kaskaoutis, D.G., Ram, K., Panicker, A.S., Srivastava, M.K., Tiwari, S., Attri, S.D., Soni, V.K., Pandey, A.K.: Aerosol chemical characterization and role of carbonaceous aerosol on radiative effect over Varanasi in central Indo-Gangetic Plain. Atmos Environ. **125**, 437–449 (2016)

Turpin, B.J., Huntzicker, J.J.: Identification of secondary organic aerosol episodes and quantification of primary and secondary organic aerosol concentrations during SCAQS. Atmos Environ. **23**, 3527–3544 (1995)

Vadrevu, K.P., Ellicott, E., Giglio, L., Badarinath, K.V.S., Vermote, E., Justice, C., Lau, W.K.M.: Vegetation fires in the Himalayan region—aerosol load, black carbon emissions and smoke plume heights. Atmos Environ. **47**, 241–251 (2012)

Valenzuela, A., Olmo, F.J., Lyamani, H., Antón, M., Titos, G., Cazorla, A., Alados-Arboledas, L.: Aerosol scattering and absorption Angström exponents as indicators of dust and dust-free days over Granada (Spain). Atmos Res. **154**, 1–13 (2015)

Venkataraman, C., Habib, G., Eiguren Fernandez, A., Miguel, A.H., Friedlander, S.K.: Residential biofuels in South Asia: carbonaceous aerosol emissions and climate impacts. Science. **307**, 1454–1456 (2005)

Viana, M., Maenhaut, W., Ten Brink, H.M., Chi, X., Weijers, E., Querol, X., Alastuey, A., Mikuska., P., Vecera, Z.: Comparative analysis of organic and elemental carbon concentrations in carbonaceous aerosols in three European cities. Atmos Environ. **41**, 5972–5983 (2007)

Wang, B., Shi, G.: Long-term trends of atmospheric absorbing and scattering optical depths over China region estimated from the routine observation data of surface solar irradiances. J Geophys Res. **115**, D00K28 (2010). doi:10.1029/2009JD013239

Wang, X., Ding, X., Fu, X., He, Q., Wang, S., Bernard, F., Zhao, X., Wu, D.: Aerosol scattering coefficients and major chemical compositions of fine particles observed at a rural site in the central Pearl River Delta. South China J Environ Sci. **24**, 72–77 (2012)

Wang, L., Salazar, G.A., Gong, W., Peng, S., Zou, L., Lin, A.: An improved method for estimating the Ångstrom turbidity coefficient β in Central China during 1961-2010. Energy. **81**, 67–73 (2015)

Zhang, F., Chen, J., Qiu, T., Yin, L., Chen, X., Yu, J.: Pollution Characteristics of $PM_{2.5}$ during a Typical Haze Episode in Xiamen, China. Atmos Clim Sci. **3**, 427–439 (2013a)

Zhang, G., Bi, X., Chan, L., Wang, X., Sheng, G., Fu, J.: Size-segregated chemical characteristics of aerosol during haze in an urban area of the Pearl River Delta region. China Urban Clim. **4**, 74–84 (2013b)